Physical interpretation of the baryon spectrum

Derek Leinweber

Key collaborators: Curtis Abell, Liam Hockley, Waseem Kamleh, Zhan-Wei Liu, Finn Stokes, Tony Thomas, Jia-Jun Wu

SPECIAL RESEARCH CENTRE FOR THE SUBATOMIC STRUCTURE OF MATTER

THE UNIVERSITY of ADELAIDE

Closely related presentations this week

- **The study of N*(1535) and N*(1650) from the lattice data** (14:50)
  Presenter: Jia-jun Wu (University of Chinese Academy of Science)
  Parallel Session: I B - Walmgate Suite (Monday 17 June 2024, 13:30 - 15:15)

- **Three particle interactions on the lattice** (10:00)
  Presenter: Maxim Mai (University of Bonn / The George Washington University)
  Plenary Session: V - (Wednesday 19 June 2024, 09:00 - 10:30)

Prologue

- The idea of dressing quark-model states in a coupled-channel analysis to describe scattering data has been around for decades.

Prologue

- The idea of dressing quark-model states in a coupled-channel analysis to describe scattering data has been around for decades.
- What's new are formalisms able to bring these descriptions to the finite-volume of lattice QCD.

Prologue

- The idea of dressing quark-model states in a coupled-channel analysis to describe scattering data has been around for decades.
- What's new are formalisms able to bring these descriptions to the finite-volume of lattice QCD.
- Lattice QCD calculations of the excitation spectrum provide new constraints.

Prologue

- The idea of dressing quark-model states in a coupled-channel analysis to describe scattering data has been around for decades.
- What's new are formalisms able to bring these descriptions to the finite-volume of lattice QCD.
- Lattice QCD calculations of the excitation spectrum provide new constraints.
- It's time to reconsider our early notions about the quark-model and its excitation spectrum.

Accessing the Radial Excitations of the Nucleon - CSSM Techniques

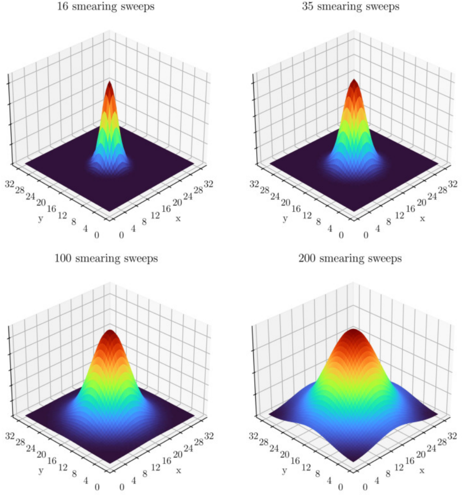

- Circa 2010.
- Local 3-quark interpolating fields.
- Quark-level source smearing techniques.

Accessing the Radial Excitations of the Nucleon - CSSM Techniques

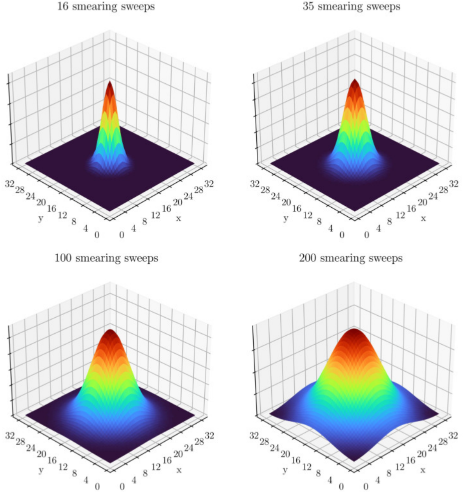

- Circa 2010.
- Local 3-quark interpolating fields.
- Quark-level source smearing techniques.
- Correlation matrix techniques
  - Identify linear combinations of sources to isolate states.
  - Opposite sign superpositions create wave function nodes.

Δ Baryon Interpolating Field Shapes

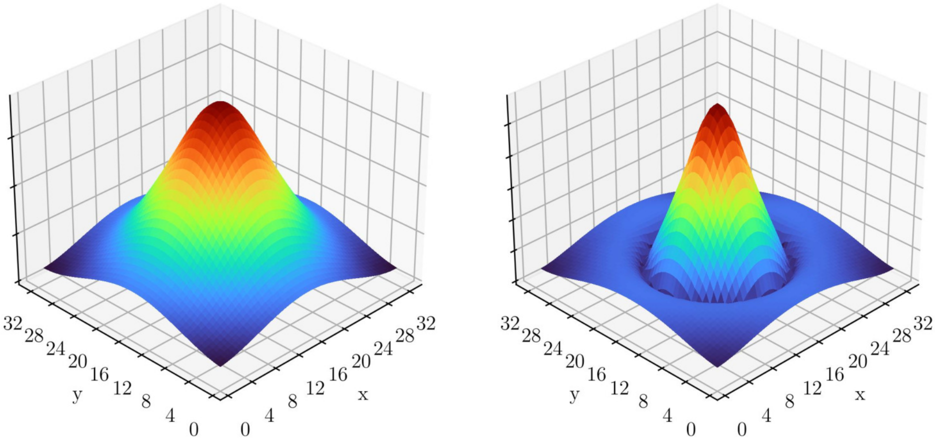

Δ-baryon spectrum from lattice QCD – $1s$ and $2s$ excitations

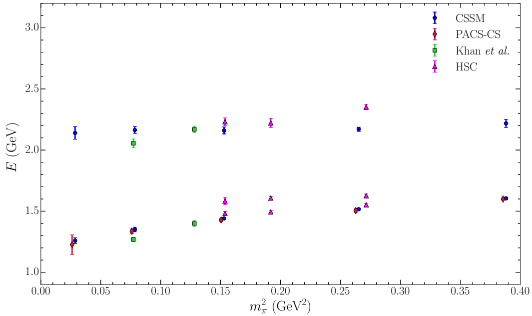

CSSM: L. Hockley, *et al.*, J. Phys. G **51** (2024) no.6, 065106 [arXiv:2312.11574 [hep-lat]].

Kahn ***et al.*****:** T. Khan, D. Richards and F. Winter, Phys. Rev. D **104** (2021) 034503 [arXiv:2010.03052 [hep-lat]].

HSC: J. Bulava, *et al.*, Phys. Rev. D **82** (2010) 014507 [arXiv:1004.5072 [hep-lat]].

PACS-CS: S. Aoki *et al.* [PACS-CS], Phys. Rev. D **79** (2009) 034503 [arXiv:0807.1661 [hep-lat]].

Where's the $\Delta(1600)$ – the Roper-like resonance?

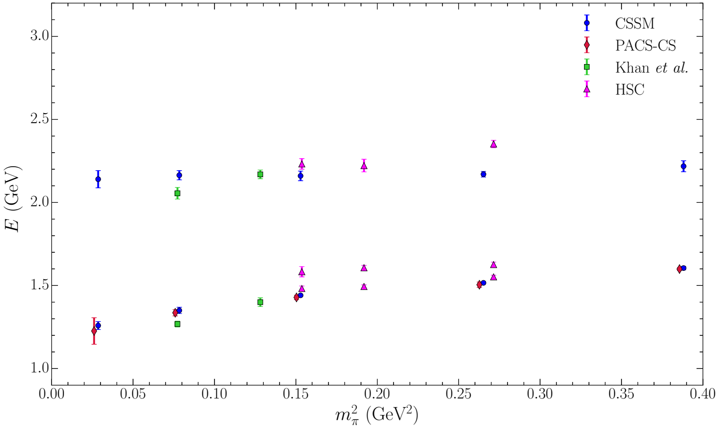

- Roper-like: 1st even-parity excitation sits below the 1st odd-parity, $\Delta(1700)$.

Positive Parity Nucleon Spectrum Circa 2017

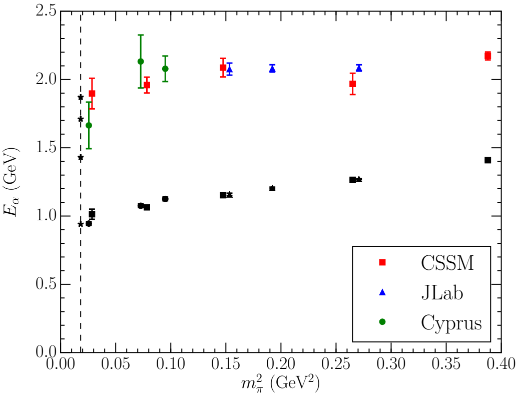

- **CSSM:** Z. W. Liu, *et al.* [CSSM], Phys. Rev. D **95**, 034034 (2017) arXiv:1607.04536 [nucl-th]
- **JLab:** R. G. Edwards, *et al.* [HSC] Phys. Rev. D **84**, 074508 (2011) [arXiv:1104.5152 [hep-ph]].
- **Cyprus:** C. Alexandrou, *et al.* (AMIAS), Phys. Rev. D **91**, 014506 (2015) arXiv:1411.6765 [hep-lat]

Landau-Gauge Wave functions from the Lattice

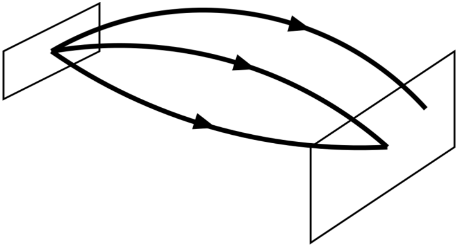

- Measure the *overlap* of the annihilation operator with the state as a function of the quark positions.

d-quark probability density in ground state proton [CSSM]

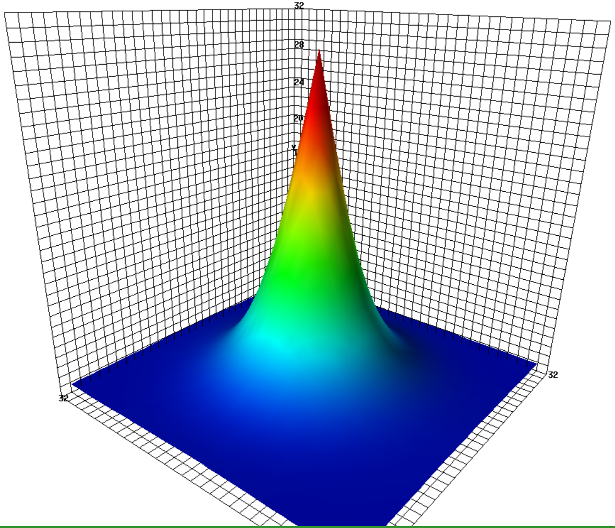

d-quark probability density in the 1st excited state of proton [CSSM]

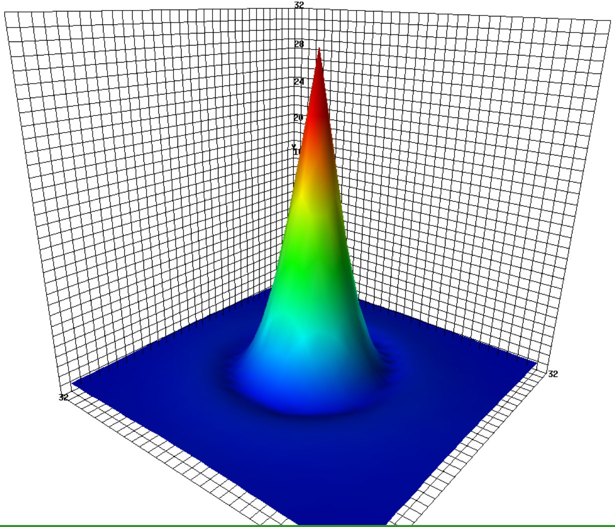

d-quark probability density in the 2nd excited state of proton [CSSM]

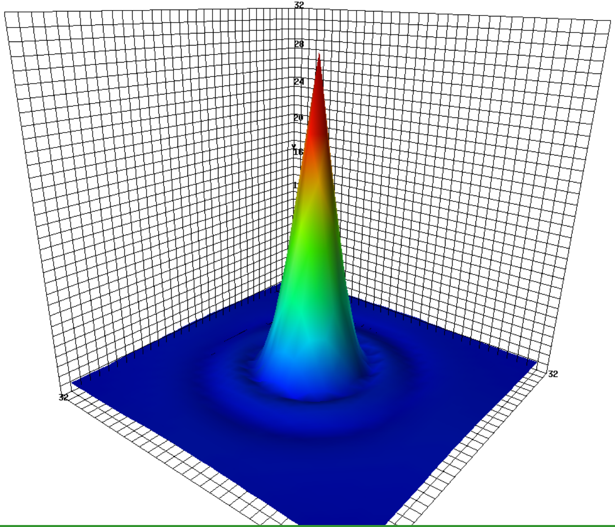

Comparison with the Simple Quark Model [CSSM]

D. S. Roberts, W. Kamleh and D. B. Leinweber, Phys. Lett. B **725**, 164 (2013) [arXiv:1304.0325 [hep-lat]].

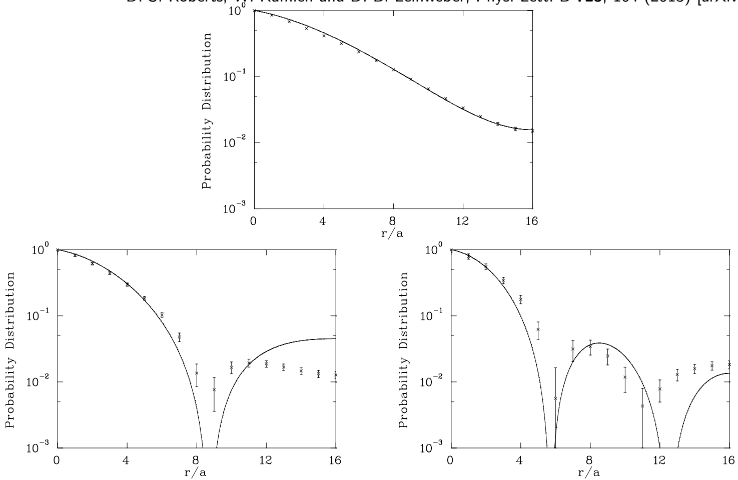

First positive-parity excitation: Magnetic moments

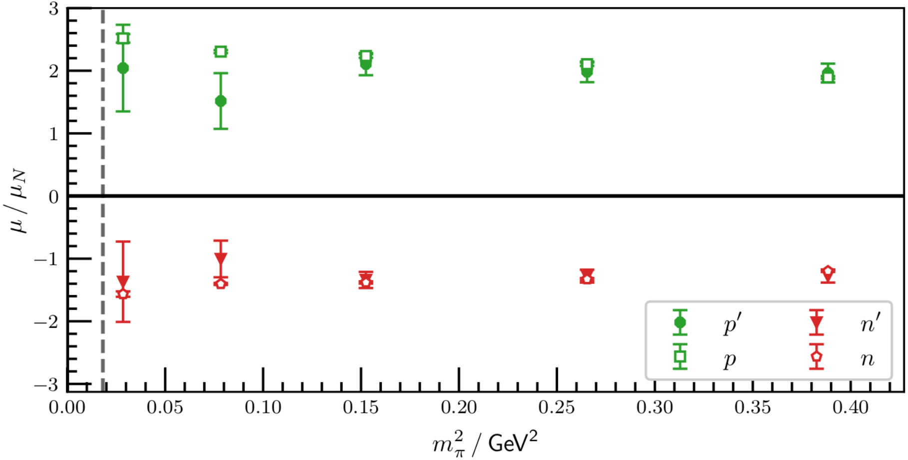

F. M. Stokes, W. Kamleh, DBL, Phys. Rev. D **102** (2020) 014507 [arXiv:1907.00177 [hep-lat]].

The spectrum of a simple quark model: N and Λ baryons

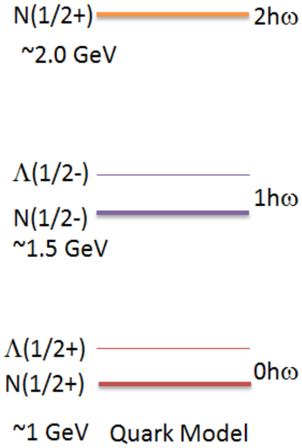

The challenge of experiment

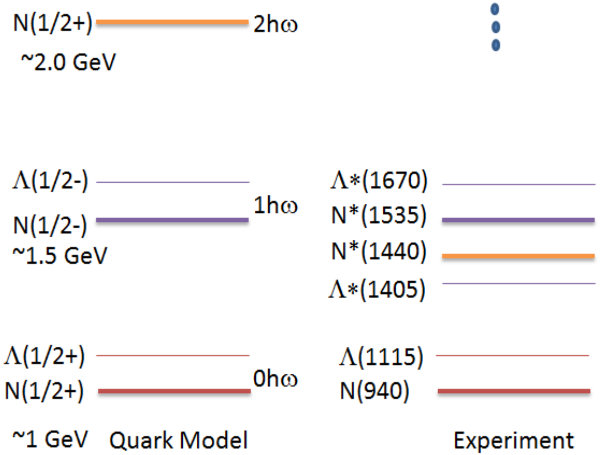

The spectrum of quark-model-like states is relatively simple

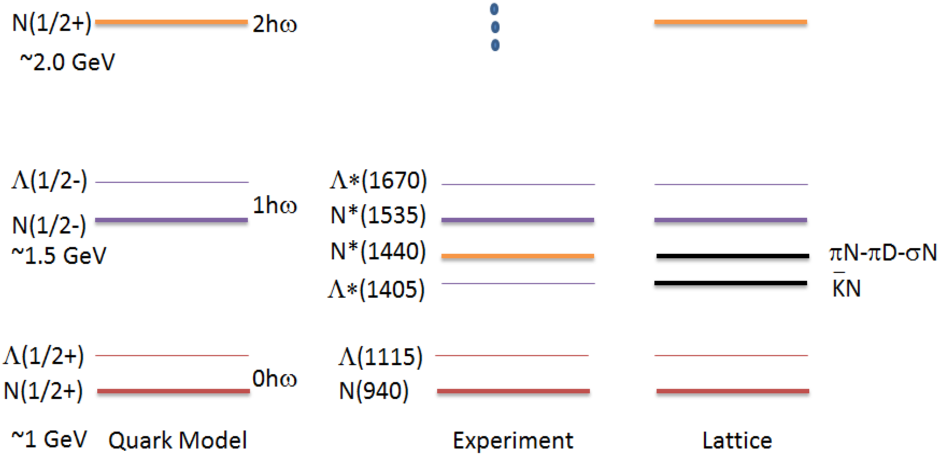

Outline

- Hamiltonian Effective Field Theory (HEFT)
  - Coupled-channel analysis technique aimed at resonance physics.
  - Incorporates the Lüscher formalism.
  - Connects scattering observables to the finite-volume spectrum of lattice QCD.

Outline

- Hamiltonian Effective Field Theory (HEFT)
  - Coupled-channel analysis technique aimed at resonance physics.
  - Incorporates the Lüscher formalism.
  - Connects scattering observables to the finite-volume spectrum of lattice QCD.
- New analysis of $\Delta\frac{3}{2}^+$ resonances aimed at describing the $\Delta(1600)$ and $\Delta(1920)$.
  - Discuss the composition of excited states.
  - Confront state-of-the-art lattice QCD calculations of the scattering-state spectrum.

Outline

- Hamiltonian Effective Field Theory (HEFT)
  - Coupled-channel analysis technique aimed at resonance physics.
  - Incorporates the Lüscher formalism.
  - Connects scattering observables to the finite-volume spectrum of lattice QCD.
- New analysis of $\Delta\frac{3}{2}^+$ resonances aimed at describing the $\Delta(1600)$ and $\Delta(1920)$.
  - Discuss the composition of excited states.
  - Confront state-of-the-art lattice QCD calculations of the scattering-state spectrum.
- New analysis of $\Lambda\frac{1}{2}^-$ resonances aimed at describing the $\Lambda(1405)$ and $\Lambda(1670)$.
  - Draws on recent advances in experiment.
  - Confront new lattice QCD spectra from the Baryon Scattering (BaSc) Collaboration.

Outline

- Hamiltonian Effective Field Theory (HEFT)
  - Coupled-channel analysis technique aimed at resonance physics.
  - Incorporates the Lüscher formalism.
  - Connects scattering observables to the finite-volume spectrum of lattice QCD.
- New analysis of $\Delta\frac{3}{2}^+$ resonances aimed at describing the $\Delta(1600)$ and $\Delta(1920)$.
  - Discuss the composition of excited states.
  - Confront state-of-the-art lattice QCD calculations of the scattering-state spectrum.
- New analysis of $\Lambda\frac{1}{2}^-$ resonances aimed at describing the $\Lambda(1405)$ and $\Lambda(1670)$.
  - Draws on recent advances in experiment.
  - Confront new lattice QCD spectra from the Baryon Scattering (BaSc) Collaboration.
- Roper $N\frac{1}{2}^+(1440)$ resonance.

Outline

- Hamiltonian Effective Field Theory (HEFT)
  - Coupled-channel analysis technique aimed at resonance physics.
  - Incorporates the Lüscher formalism.
  - Connects scattering observables to the finite-volume spectrum of lattice QCD.
- New analysis of $\Delta\frac{3}{2}^+$ resonances aimed at describing the $\Delta(1600)$ and $\Delta(1920)$.
  - Discuss the composition of excited states.
  - Confront state-of-the-art lattice QCD calculations of the scattering-state spectrum.
- New analysis of $\Lambda\frac{1}{2}^-$ resonances aimed at describing the $\Lambda(1405)$ and $\Lambda(1670)$.
  - Draws on recent advances in experiment.
  - Confront new lattice QCD spectra from the Baryon Scattering (BaSc) Collaboration.
- Roper $N\frac{1}{2}^+(1440)$ resonance.
- A new resolution of the missing baryon resonances problem.

Section 2

Hamiltonian Effective Field Theory (HEFT)

Hamiltonian Effective Field Theory (HEFT)

J. M. M. Hall, *et al.* [CSSM], Phys. Rev. D **87** (2013) 094510 [arXiv:1303.4157 [hep-lat]]

C. D. Abell, DBL, A. W. Thomas, J. J. Wu, Phys. Rev. D **106** (2022) 034506 [arXiv:2110.14113 [hep-lat]]

- An extension of chiral effective field theory incorporating the Lüscher formalism
  - Linking the energy levels observed in finite volume to scattering observables.

Hamiltonian Effective Field Theory (HEFT)

J. M. M. Hall, *et al.* [CSSM], Phys. Rev. D **87** (2013) 094510 [arXiv:1303.4157 [hep-lat]]

C. D. Abell, DBL, A. W. Thomas, J. J. Wu, Phys. Rev. D **106** (2022) 034506 [arXiv:2110.14113 [hep-lat]]

- An extension of chiral effective field theory incorporating the Lüscher formalism
  - Linking the energy levels observed in finite volume to scattering observables.
- In the light quark-mass regime, in the perturbative limit,
  - HEFT reproduces the finite-volume expansion of chiral perturbation theory.

Hamiltonian Effective Field Theory (HEFT)

J. M. M. Hall, *et al.* [CSSM], Phys. Rev. D **87** (2013) 094510 [arXiv:1303.4157 [hep-lat]]

C. D. Abell, DBL, A. W. Thomas, J. J. Wu, Phys. Rev. D **106** (2022) 034506 [arXiv:2110.14113 [hep-lat]]

- An extension of chiral effective field theory incorporating the Lüscher formalism
  - Linking the energy levels observed in finite volume to scattering observables.
- In the light quark-mass regime, in the perturbative limit,
  - HEFT reproduces the finite-volume expansion of chiral perturbation theory.
- Fitting resonance phase-shift data and inelasticities,
  - Predictions of the finite-volume spectrum are made.

Hamiltonian Effective Field Theory (HEFT)

J. M. M. Hall, *et al.* [CSSM], Phys. Rev. D **87** (2013) 094510 [arXiv:1303.4157 [hep-lat]]

C. D. Abell, DBL, A. W. Thomas, J. J. Wu, Phys. Rev. D **106** (2022) 034506 [arXiv:2110.14113 [hep-lat]]

- An extension of chiral effective field theory incorporating the Lüscher formalism
  - Linking the energy levels observed in finite volume to scattering observables.
- In the light quark-mass regime, in the perturbative limit,
  - HEFT reproduces the finite-volume expansion of chiral perturbation theory.
- Fitting resonance phase-shift data and inelasticities,
  - Predictions of the finite-volume spectrum are made.
- The eigenvectors of the Hamiltonian provide insight into the composition of the energy eigenstates.
  - Insight is similar to that provided by correlation-matrix eigenvectors in Lattice QCD.

Infinite Volume Model

- The rest-frame Hamiltonian has the form $H = H_0 + H_I$, with

$$H_0 = \sum_{B_0} |B_0\rangle \, m_{B_0} \, \langle B_0| + \sum_{\alpha} \int d^3k \, |\alpha(\boldsymbol{k})\rangle \, \omega_\alpha(\boldsymbol{k}) \, \langle \alpha(\boldsymbol{k})| \, ,$$

Infinite Volume Model

- The rest-frame Hamiltonian has the form $H = H_0 + H_I$, with

$$H_0 = \sum_{B_0} |B_0\rangle \, m_{B_0} \, \langle B_0| + \sum_{\alpha} \int d^3k \, |\alpha(\boldsymbol{k})\rangle \, \omega_\alpha(\boldsymbol{k}) \, \langle \alpha(\boldsymbol{k})| \, ,$$

- $|B_0\rangle$ denotes a quark-model-like basis state with bare mass m_{B_0}.

Infinite Volume Model

- The rest-frame Hamiltonian has the form $H = H_0 + H_I$, with

$$H_0 = \sum_{B_0} |B_0\rangle \, m_{B_0} \, \langle B_0| + \sum_{\alpha} \int d^3k \, |\alpha(\boldsymbol{k})\rangle \, \omega_\alpha(\boldsymbol{k}) \, \langle \alpha(\boldsymbol{k})| \, ,$$

- $|B_0\rangle$ denotes a quark-model-like basis state with bare mass m_{B_0}.
- $|\alpha(\boldsymbol{k})\rangle$ designates a two-particle non-interacting basis-state channel with energy

$$\omega_\alpha(\boldsymbol{k}) = \omega_{\alpha_M}(\boldsymbol{k}) + \omega_{\alpha_B}(\boldsymbol{k}) = \sqrt{\boldsymbol{k}^2 + m_{\alpha_M}^2} + \sqrt{\boldsymbol{k}^2 + m_{\alpha_B}^2} \, ,$$

for $M =$ Meson, $B =$ Baryon.

Infinite Volume Model

- The interaction Hamiltonian includes two parts, $H_I = g + v$.
- $1 \to 2$ particle vertex

$$g = \sum_{\alpha,\, B_0} \int d^3k \, \left\{ |\alpha(\boldsymbol{k})\rangle \, G^\dagger_{\alpha,B_0}(k) \, \langle B_0| + h.c. \right\} ,$$

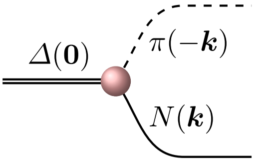

Infinite Volume Model

- The interaction Hamiltonian includes two parts, $H_I = g + v$.
- $1 \to 2$ particle vertex

$$g = \sum_{\alpha,\, B_0} \int d^3k \, \left\{ |\alpha(\boldsymbol{k})\rangle \, G^{\dagger}_{\alpha,B_0}(k) \, \langle B_0| + h.c. \right\} \, ,$$

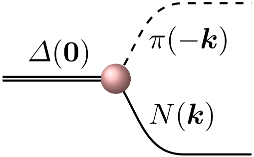

- $2 \to 2$ particle vertex

$$v = \sum_{\alpha,\beta} \int d^3k \; d^3k' \, |\alpha(\boldsymbol{k})\rangle \, V^S_{\alpha,\beta}(k,k') \, \langle \beta(\boldsymbol{k}')| \, .$$

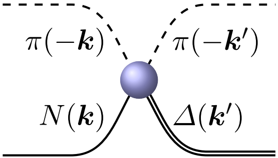

S-wave vertex interactions

- S-wave one to two-particle interactions take the form

$$G_{\alpha,B_0}(k) = g_{B_0\alpha}\,\frac{\sqrt{3}}{2\,\pi\,f_\pi}\,\sqrt{\omega_{\alpha_M}(k)}\,u(k,\Lambda)\,,$$

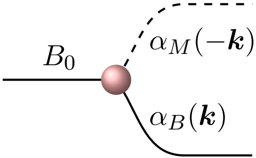

with dipole regulator

$$u(k,\Lambda) = \frac{1}{\left(1 + k^2/\Lambda^2\right)^2}\,.$$

P-wave and higher vertex interactions

- P-wave and higher vertex interactions take the form

$$G_{\alpha,B_0}(k) = g_{B_0\alpha}\,\frac{1}{4\pi^2}\left(\frac{k}{f_\pi}\right)^{l_\alpha}\frac{u(k,\Lambda)}{\sqrt{\omega_{\alpha_M}(k)}}\,,$$

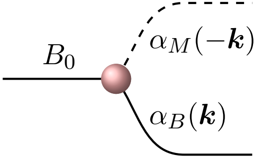

where l_α is the orbital angular momentum in channel α.

Two-to-two particle interactions

- For S-wave scattering

$$V^{S}_{\alpha,\beta}\,(\,k,\;k'\,) = v_{\alpha,\beta}\,\frac{3}{4\pi^2\,f_\pi^2}\,u(k,\mathit{\Lambda})\,u(k',\mathit{\Lambda})$$

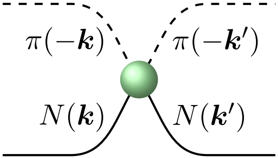

with dipole regulator

$$u(k,\mathit{\Lambda}) = \frac{1}{(\,1 + k^2/\mathit{\Lambda}^2\,)^2}\,.$$

Two-to-two particle interactions

- For P-wave scattering in the N^* and Δ channels

$$V^{S}_{\alpha,\beta}\,(\,k,\,k'\,) = v_{\alpha,\beta}\,\frac{1}{4\pi^2\,f_\pi^2}\,\frac{k}{\omega_{\alpha_M}(k)}\,\frac{k'}{\omega_{\beta_M}(k')}\,u(k,\Lambda)\,u(k',\Lambda)\,.$$

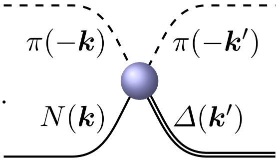

Two-to-two particle interactions

- For P-wave scattering in the N^* and Δ channels

$$V^S_{\alpha,\beta}(\,k,\,k'\,) = v_{\alpha,\beta}\,\frac{1}{4\pi^2\,f_\pi^2}\,\frac{k}{\omega_{\alpha_M}(k)}\,\frac{k'}{\omega_{\beta_M}(k')}\,u(k,\Lambda)\,u(k',\Lambda)\,.$$

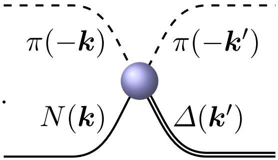

- For the $\Lambda^*(1405)$, the Weinberg-Tomozawa form is considered

$$V^S_{\alpha,\beta}(\,k,\,k'\,) = v^{\Lambda^*}_{\alpha,\beta}\,\frac{[\,\omega_{\alpha_M}(k)+\omega_{\beta_M}(k')\,]\,u(k,\Lambda)\,u(k',\Lambda)}{16\,\pi^2\,f_\pi^2\sqrt{\omega_{\alpha_M}(k)\,\omega_{\beta_M}(k')}}\,,$$

Infinite-Volume scattering amplitude

- The T-matrices for two particle scattering are obtained by solving the coupled-channel integral equations

$$T_{\alpha,\beta}(k,k';E) = \tilde{V}_{\alpha,\beta}(k,k';E) + \sum_{\gamma} \int q^2 dq \, \frac{\tilde{V}_{\alpha,\gamma}(k,q;E)\, T_{\gamma,\beta}(q,k';E)}{E - \omega_{\gamma}(q) + i\epsilon} \, .$$

Infinite-Volume scattering amplitude

- The T-matrices for two particle scattering are obtained by solving the coupled-channel integral equations

$$T_{\alpha,\beta}(k,k';E) = \tilde{V}_{\alpha,\beta}(k,k';E) + \sum_{\gamma} \int q^2 dq \, \frac{\tilde{V}_{\alpha,\gamma}(k,q;E)\, T_{\gamma,\beta}(q,k';E)}{E - \omega_{\gamma}(q) + i\epsilon} \, .$$

- The coupled-channel potential is readily calculated from the interaction Hamiltonian

$$\tilde{V}_{\alpha,\beta}(k,k') = \sum_{B_0} \frac{G^{\dagger}_{\alpha,B_0}(k)\, G_{\beta,B_0}(k')}{E - m_{B_0}} + V^{S}_{\alpha,\beta}(k,k') \, ,$$

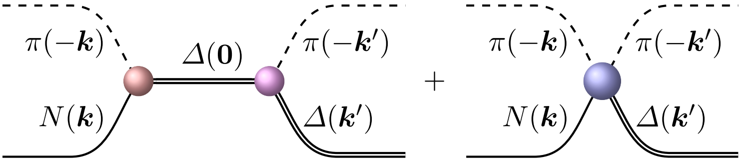

Infinite-Volume scattering matrix

- The S-matrix is related to the T-matrix by

$$S_{\alpha,\beta}(E) = 1 - 2i\,\sqrt{\rho_\alpha(E)\,\rho_\beta(E)}\;T_{\alpha,\beta}(k_{\alpha\,\mathrm{cm}}, k_{\beta\,\mathrm{cm}}; E)\,,$$

with

$$\rho_\alpha(E) = \pi\,\frac{\omega_{\alpha_M}(k_{\alpha\,\mathrm{cm}})\,\omega_{\alpha_B}(k_{\alpha\,\mathrm{cm}})}{E}\,k_{\alpha\,\mathrm{cm}}\,,$$

and $k_{\alpha\,\mathrm{cm}}$ satisfies the on-shell condition

$$\omega_{\alpha_M}(k_{\alpha\,\mathrm{cm}}) + \omega_{\alpha_B}(k_{\alpha\,\mathrm{cm}}) = E\,.$$

Infinite-Volume scattering matrix

- The S-matrix is related to the T-matrix by

$$S_{\alpha,\beta}(E) = 1 - 2i\,\sqrt{\rho_\alpha(E)\,\rho_\beta(E)}\;T_{\alpha,\beta}(k_{\alpha\,\mathrm{cm}}, k_{\beta\,\mathrm{cm}}; E)\,,$$

with

$$\rho_\alpha(E) = \pi\,\frac{\omega_{\alpha_M}(k_{\alpha\,\mathrm{cm}})\,\omega_{\alpha_B}(k_{\alpha\,\mathrm{cm}})}{E}\;k_{\alpha\,\mathrm{cm}}\,,$$

and $k_{\alpha\,\mathrm{cm}}$ satisfies the on-shell condition

$$\omega_{\alpha_M}(k_{\alpha\,\mathrm{cm}}) + \omega_{\alpha_B}(k_{\alpha\,\mathrm{cm}}) = E\,.$$

- The cross section $\sigma_{\alpha\,,\beta}$ for the process $\alpha \to \beta$ is

$$\sigma_{\alpha\,,\beta} = \frac{4\pi^3\,k_{\alpha\,\mathrm{cm}}\,\omega_{\alpha_M}(k_{\alpha\,\mathrm{cm}})\,\omega_{\alpha_B}(k_{\alpha\,\mathrm{cm}})\,\omega_{\beta_M}(k_{\alpha\,\mathrm{cm}})\,\omega_{\beta_B}(k_{\alpha\,\mathrm{cm}})}{E^2\,k_{\beta\,\mathrm{cm}}}\;|T_{\alpha,\beta}(k_{\alpha\,\mathrm{cm}}, k_{\beta\,\mathrm{cm}}; E)|^2\;.$$

πN phase shift and inelasticity

- The S-matrix is related to the T-matrix by

$$\begin{aligned} S_{\pi N,\pi N}(E) &= 1 - 2i\pi \frac{\omega_\pi(k_{\rm cm})\,\omega_N(k_{\rm cm})}{E}\, k_{\rm cm}\; T_{\pi N,\pi N}(k_{\rm cm}, k_{\rm cm}; E)\,, \\ &= \eta(E)\, e^{2i\,\delta(E)}\,. \end{aligned}$$

- In solving the integral equations...

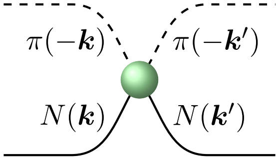

πN phase shift and inelasticity

- The S-matrix is related to the T-matrix by

$$
\begin{aligned}
S_{\pi N,\pi N}(E) &= 1 - 2i\pi \, \frac{\omega_\pi(k_{\rm cm})\,\omega_N(k_{\rm cm})}{E}\, k_{\rm cm}\; T_{\pi N,\pi N}(k_{\rm cm}, k_{\rm cm}; E)\,, \\
&= \eta(E)\, e^{2i\,\delta(E)}\,.
\end{aligned}
$$

- In solving the integral equations. . .

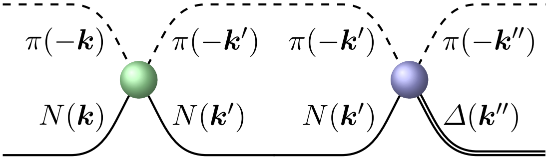

πN phase shift and inelasticity

- The S-matrix is related to the T-matrix by

$$
\begin{aligned}
S_{\pi N,\pi N}(E) &= 1 - 2i\pi \, \frac{\omega_\pi(k_{\rm cm})\, \omega_N(k_{\rm cm})}{E} \, k_{\rm cm} \; T_{\pi N,\pi N}(k_{\rm cm}, k_{\rm cm}; E)\,, \\
&= \eta(E)\, e^{2i\,\delta(E)}\,.
\end{aligned}
$$

- In solving the integral equations…

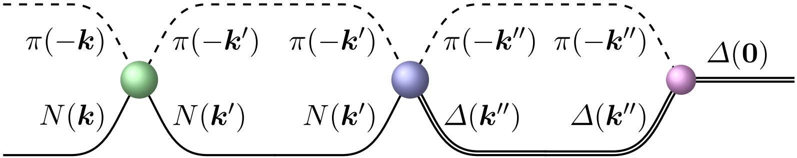

πN phase shift and inelasticity

- The S-matrix is related to the T-matrix by

$$
\begin{aligned}
S_{\pi N,\pi N}(E) &= 1 - 2i\pi\,\frac{\omega_\pi(k_{\rm cm})\,\omega_N(k_{\rm cm})}{E}\,k_{\rm cm}\;T_{\pi N,\pi N}(k_{\rm cm},k_{\rm cm};E)\,,\\
&= \eta(E)\,e^{2i\,\delta(E)}\,.
\end{aligned}
$$

- In solving the integral equations...

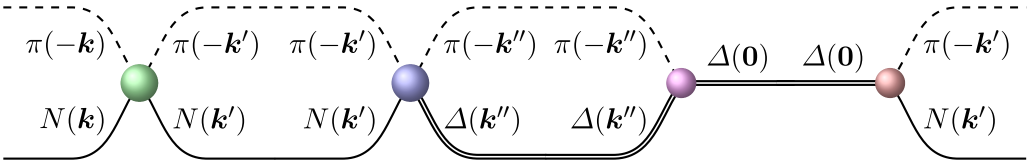

Fit to Scattering Data in the Δ-Resonance Channel

- Consider:
  - p-wave πN,
  - p-wave $\pi\Delta$, and
  - f-wave $\pi\Delta$

  channels, dressing
  - two bare basis states.
- Fit to SAID data.

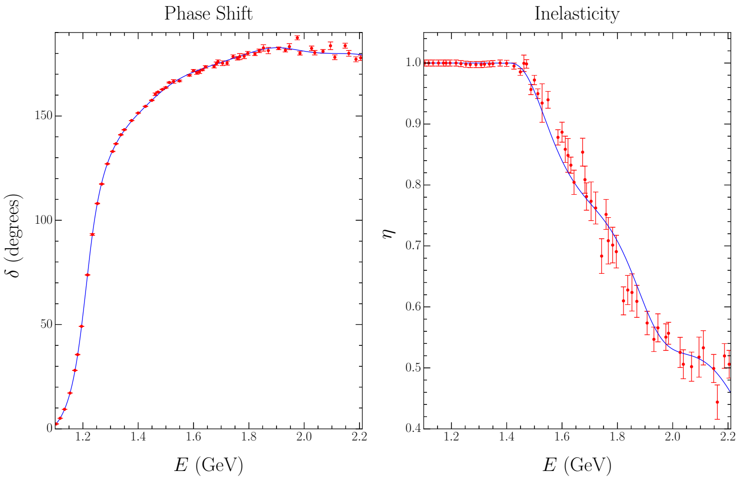

L. Hockley, C. Abell, DBL, and A. Thomas, [arXiv:2406.00981 [hep-ph]].

Pole Positions for $\Delta(1232)$, $\Delta(1600)$, and $\Delta(1920)$

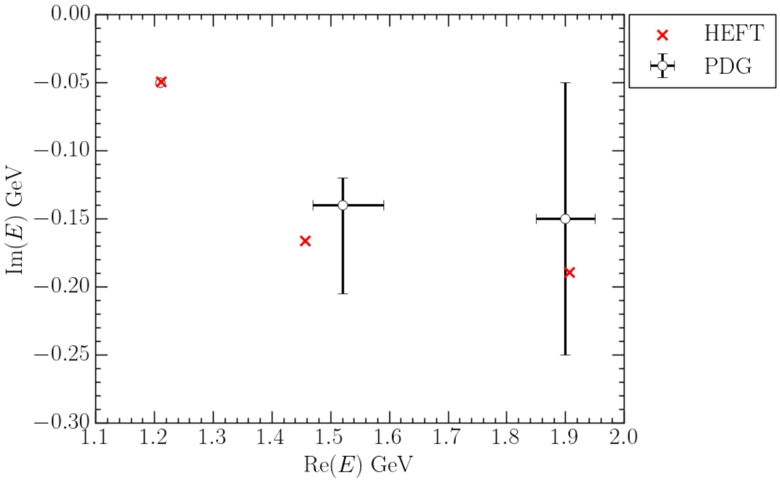

Finite Volume Analysis - Hamiltonian Matrix

- In a finite periodic volume, momentum is quantised to $n\,(2\pi/L)$.

Finite Volume Analysis - Hamiltonian Matrix

- In a finite periodic volume, momentum is quantised to $n\,(2\pi/L)$.
- In a cubic volume of extent L on each side, define the momentum magnitudes

$$k_n = \sqrt{n_x^2 + n_y^2 + n_z^2}\,\frac{2\pi}{L}\,,$$

with $n_i = 0, \pm 1, \pm 2, \ldots$ and integer $n = n_x^2 + n_y^2 + n_z^2$.

Finite Volume Analysis - Hamiltonian Matrix

- In a finite periodic volume, momentum is quantised to $n\,(2\pi/L)$.
- In a cubic volume of extent L on each side, define the momentum magnitudes

$$k_n = \sqrt{n_x^2 + n_y^2 + n_z^2}\,\frac{2\pi}{L}\,,$$

  with $n_i = 0, \pm 1, \pm 2, \ldots$ and integer $n = n_x^2 + n_y^2 + n_z^2$.
- The degeneracy of each k_n is described by $C_3(n)$, which counts the number of ways the integers n_x, n_y, and n_z, can be squared and summed to n.

Finite Volume Analysis - Hamiltonian Matrix

- In a finite periodic volume, momentum is quantised to $n\,(2\pi/L)$.
- In a cubic volume of extent L on each side, define the momentum magnitudes

$$k_n = \sqrt{n_x^2 + n_y^2 + n_z^2}\,\frac{2\pi}{L}\,,$$

  with $n_i = 0, \pm 1, \pm 2, \ldots$ and integer $n = n_x^2 + n_y^2 + n_z^2$.
- The degeneracy of each k_n is described by $C_3(n)$, which counts the number of ways the integers n_x, n_y, and n_z, can be squared and summed to n.
- The non-interacting Hamiltonian takes the form

$$H_0 = \mathrm{diag}\left(m_{\Delta_1}, m_{\Delta_2}, \omega_{\pi N}(k_1), \omega_{\pi\Delta}(k_1), \ldots, \omega_{\pi N}(k_{n_{\mathrm{max}}}), \omega_{\pi\Delta}(k_{n_{\mathrm{max}}})\right)\,.$$

Interaction Hamiltonian Terms

- $1 \to 2$ particle interaction terms sit in the first rows and columns.

$$H_I = \begin{pmatrix} 0 & 0 & \bar{G}^{\Delta_1}_{\pi N}(k_1) & \bar{G}^{\Delta_1}_{\pi \Delta}(k_1) & \bar{G}^{\Delta_1}_{\pi N}(k_2) & \bar{G}^{\Delta_1}_{\pi \Delta}(k_2) & \ldots & \bar{G}^{\Delta_1}_{\pi N}(k_{n_{\mathsf{max}}}) & \bar{G}^{\Delta_1}_{\pi \Delta}(k_{n_{\mathsf{max}}}) \\ 0 & 0 & \bar{G}^{\Delta_2}_{\pi N}(k_1) & \bar{G}^{\Delta_2}_{\pi \Delta}(k_1) & \bar{G}^{\Delta_2}_{\pi N}(k_2) & \bar{G}^{\Delta_2}_{\pi \Delta}(k_2) & \ldots & \bar{G}^{\Delta_2}_{\pi N}(k_{n_{\mathsf{max}}}) & \bar{G}^{\Delta_2}_{\pi \Delta}(k_{n_{\mathsf{max}}}) \\ \bar{G}^{\Delta_1}_{\pi N}(k_1) & \bar{G}^{\Delta_2}_{\pi N}(k_1) & & & & & & & \\ \bar{G}^{\Delta_1}_{\pi \Delta}(k_1) & \bar{G}^{\Delta_2}_{\pi \Delta}(k_1) & & & & & & & \\ \bar{G}^{\Delta_1}_{\pi N}(k_2) & \bar{G}^{\Delta_2}_{\pi N}(k_2) & & & & & & & \\ \bar{G}^{\Delta_1}_{\pi \Delta}(k_2) & \bar{G}^{\Delta_2}_{\pi \Delta}(k_2) & & & & \bar{V}^S & & & \\ \vdots & \vdots & & & & & & & \\ \bar{G}^{\Delta_1}_{\pi N}(k_{n_{\mathsf{max}}}) & \bar{G}^{\Delta_2}_{\pi N}(k_{n_{\mathsf{max}}}) & & & & & & & \\ \bar{G}^{\Delta_1}_{\pi \Delta}(k_{n_{\mathsf{max}}}) & \bar{G}^{\Delta_2}_{\pi \Delta}(k_{n_{\mathsf{max}}}) & & & & & & & \end{pmatrix},$$

Interaction Hamiltonian Terms

- $1 \to 2$ particle interaction terms sit in the first rows and columns.

$$H_I = \begin{pmatrix} 0 & 0 & \bar{G}^{\Delta_1}_{\pi N}(k_1) & \bar{G}^{\Delta_1}_{\pi \Delta}(k_1) & \bar{G}^{\Delta_1}_{\pi N}(k_2) & \bar{G}^{\Delta_1}_{\pi \Delta}(k_2) & \dots & \bar{G}^{\Delta_1}_{\pi N}(k_{n_\text{max}}) & \bar{G}^{\Delta_1}_{\pi \Delta}(k_{n_\text{max}}) \\ 0 & 0 & \bar{G}^{\Delta_2}_{\pi N}(k_1) & \bar{G}^{\Delta_2}_{\pi \Delta}(k_1) & \bar{G}^{\Delta_2}_{\pi N}(k_2) & \bar{G}^{\Delta_2}_{\pi \Delta}(k_2) & \dots & \bar{G}^{\Delta_2}_{\pi N}(k_{n_\text{max}}) & \bar{G}^{\Delta_2}_{\pi \Delta}(k_{n_\text{max}}) \\ \bar{G}^{\Delta_1}_{\pi N}(k_1) & \bar{G}^{\Delta_2}_{\pi N}(k_1) & & & & & & & \\ \bar{G}^{\Delta_1}_{\pi \Delta}(k_1) & \bar{G}^{\Delta_2}_{\pi \Delta}(k_1) & & & & & & & \\ \bar{G}^{\Delta_1}_{\pi N}(k_2) & \bar{G}^{\Delta_2}_{\pi N}(k_2) & & & & & & & \\ \bar{G}^{\Delta_1}_{\pi \Delta}(k_2) & \bar{G}^{\Delta_2}_{\pi \Delta}(k_2) & & & & \bar{V}^S & & & \\ \vdots & \vdots & & & & & & & \\ \bar{G}^{\Delta_1}_{\pi N}(k_{n_\text{max}}) & \bar{G}^{\Delta_2}_{\pi N}(k_{n_\text{max}}) & & & & & & & \\ \bar{G}^{\Delta_1}_{\pi \Delta}(k_{n_\text{max}}) & \bar{G}^{\Delta_2}_{\pi \Delta}(k_{n_\text{max}}) & & & & & & & \end{pmatrix},$$

- $\bar{V}^S$ describes the $(n_c \times n_\text{max})^2$, $2 \to 2$ particle interaction terms, filling out the rest of the matrix.

Relation to infinite-volume contributions

- The finite volume Hamiltonian interaction terms are related to the infinite-volume contributions via

$$\int k^2 dk = \frac{1}{4\pi}\int d^3k \to \frac{1}{4\pi}\sum_{\boldsymbol{n}\in\mathbb{Z}^3}\left(\frac{2\pi}{L}\right)^3 = \frac{1}{4\pi}\sum_{n\in\mathbb{Z}} C_3(n)\left(\frac{2\pi}{L}\right)^3 .$$

  such that

$$\bar{G}_{\alpha,B_0}(k_n) = \sqrt{\frac{C_3(n)}{4\pi}}\left(\frac{2\pi}{L}\right)^{\frac{3}{2}} G_{\alpha,B_0}(k_n)\,,$$

$$\bar{V}^S_{\alpha\beta}(k_n,k_m) = \sqrt{\frac{C_3(n)}{4\pi}}\sqrt{\frac{C_3(m)}{4\pi}}\left(\frac{2\pi}{L}\right)^3 V^S_{\alpha\beta}(k_n,k_m)\,.$$

Finite Volume Eigenmode Solution

- Standard Lapack routines provide eigenmode solutions of

$$\langle\, i \,|\, H \,|\, j \,\rangle \,\langle\, j \,|\, E_\alpha \,\rangle = E_\alpha \,\langle\, i \,|\, E_\alpha \,\rangle \,,$$

  - where $|\, i \,\rangle$ and $|\, j \,\rangle$ are the non-interacting basis states,
  - E_α is the energy eigenvalue, and
  - $\langle\, i \,|\, E_\alpha \,\rangle$ is the eigenvector of the
  - Hamiltonian matrix $\langle\, i \,|\, H \,|\, j \,\rangle$.

Mass dependence of HEFT energy eigenstates

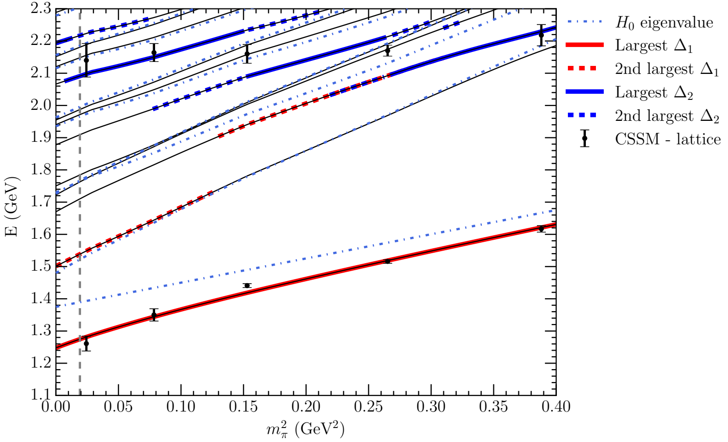

L. Hockley, C. Abell, DBL, and A. Thomas, [arXiv:2406.00981 [hep-ph]].

Mass dependence of HEFT energy eigenstates

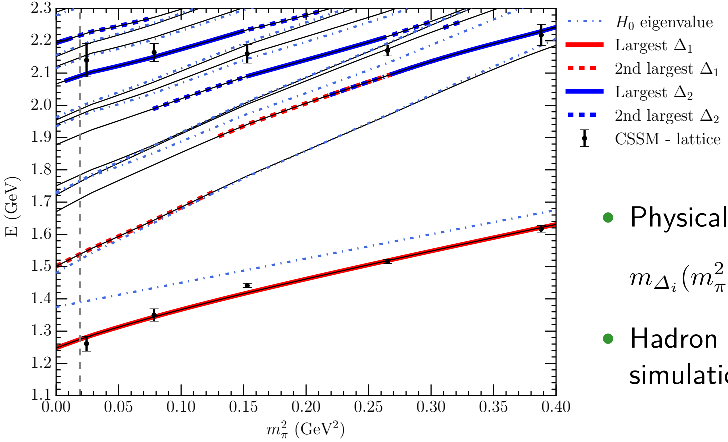

- Physical results extended via

$$m_{\Delta_i}(m_\pi^2) = m_{\Delta_i} + \alpha_{\Delta_i}\left(m_\pi^2 - m_\pi|^2_{\text{phys}}\right) .$$

- Hadron masses acquire the lattice simulation values.

L. Hockley, C. Abell, DBL, and A. Thomas, [arXiv:2406.00981 [hep-ph]].

Finite Volume Eigenmode Solution

- Standard Lapack routines provide eigenmode solutions of

$$\langle\, i \,|\, H \,|\, j \,\rangle \, \langle\, j \,|\, E_\alpha \,\rangle = E_\alpha \, \langle\, i \,|\, E_\alpha \,\rangle \,.$$

- Eigenvector $\langle\, i \,|\, E_\alpha \,\rangle$ describes the composition of the eigenstate $|\, E_\alpha \,\rangle$ in terms of the basis states $|\, i \,\rangle$ with

$$|\, i \,\rangle = |\, B_0 \,\rangle, \quad |\, \pi N, k_1 \,\rangle, \quad |\, \pi N, k_2 \,\rangle, \quad \cdots \,|\, \pi \Delta, k_1 \,\rangle, \quad |\, \pi \Delta, k_2 \,\rangle, \quad \cdots \,.$$

Finite Volume Eigenmode Solution

- Standard Lapack routines provide eigenmode solutions of

$$\langle\, i \,|\, H \,|\, j \,\rangle\, \langle\, j \,|\, E_\alpha \,\rangle = E_\alpha\, \langle\, i \,|\, E_\alpha \,\rangle\, .$$

- Eigenvector $\langle\, i \,|\, E_\alpha \,\rangle$ describes the composition of the eigenstate $|\, E_\alpha \,\rangle$ in terms of the basis states $|\, i \,\rangle$ with

$$|\, i \,\rangle = |\, B_0 \,\rangle, \quad |\, \pi N, k_1 \,\rangle, \quad |\, \pi N, k_2 \,\rangle, \quad \cdots\, |\, \pi \Delta, k_1 \,\rangle, \quad |\, \pi \Delta, k_2 \,\rangle, \quad \cdots\, .$$

- The overlap of the bare basis state $|\, B_0 \,\rangle$ with eigenstate $|\, E_\alpha \,\rangle$,

$$\langle\, B_0 \,|\, E_\alpha \,\rangle\, ,$$

is of particular interest,

Finite Volume Eigenmode Solution

- In Hamiltonian EFT, the only localised basis state is the bare basis state.

Finite Volume Eigenmode Solution

- In Hamiltonian EFT, the only localised basis state is the bare basis state.
- Bär has highlighted how χPT provides an estimate of the direct coupling of smeared nucleon interpolating fields to a non-interacting πN (basis) state,

$$\frac{3}{16}\,\frac{1}{(f_\pi\,L)^2\,E_\pi\,L}\,\left(\frac{E_N - M_N}{E_N}\right) \sim 10^{-3}\,,$$

relative to the ground state.

O. Bar, Phys. Rev. D **92** (2015) no.7, 074504 [arXiv:1503.03649 [hep-lat]].

Finite Volume Eigenmode Solution

- In Hamiltonian EFT, the only localised basis state is the bare basis state.
- Bär has highlighted how χPT provides an estimate of the direct coupling of smeared nucleon interpolating fields to a non-interacting πN (basis) state,

$$\frac{3}{16}\,\frac{1}{(f_\pi\,L)^2\,E_\pi\,L}\,\left(\frac{E_N - M_N}{E_N}\right) \sim 10^{-3}\,,$$

  relative to the ground state.

  O. Bar, Phys. Rev. D **92** (2015) no.7, 074504 [arXiv:1503.03649 [hep-lat]].

- Conclude the smeared interpolating fields of lattice QCD are associated with the bare basis states of HEFT

$$\overline{\chi}(0)\,|\Omega\rangle \simeq |B_0\rangle\ ,$$

Finite Volume Eigenmode Solution

- In Hamiltonian EFT, the only localised basis state is the bare basis state.
- Bär has highlighted how χPT provides an estimate of the direct coupling of smeared nucleon interpolating fields to a non-interacting πN (basis) state,

$$\frac{3}{16}\,\frac{1}{(f_\pi\, L)^2\, E_\pi\, L}\,\left(\frac{E_N - M_N}{E_N}\right) \sim 10^{-3}\,,$$

relative to the ground state.

O. Bar, Phys. Rev. D **92** (2015) no.7, 074504 [arXiv:1503.03649 [hep-lat]].

- Conclude the smeared interpolating fields of lattice QCD are associated with the bare basis states of HEFT

$$\overline{\chi}(0)\,|\Omega\rangle \simeq |B_0\rangle\ ,$$

- Eigenstates with large $\langle\, B_0 \,|\, E_\alpha\,\rangle$ will be excited and observed in lattice QCD.

Δ Finite Volume Spectrum at $L = 3$ fm

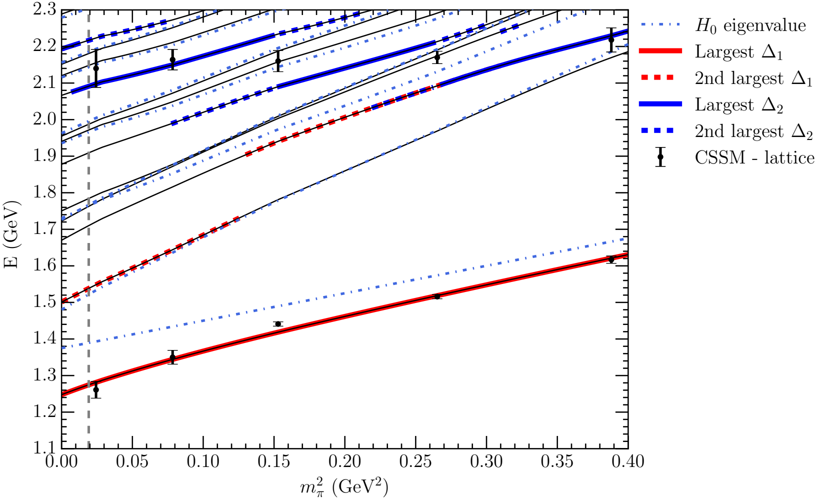

25 Fit Parameters

Parameter	Value	Parameter	Value
m_{Δ_1}/GeV	1.3894	m_{Δ_2}/GeV	2.3177
$g^{\Delta_1}_{\pi N}$	0.4974	$g^{\Delta_2}_{\pi N}$	0.2914
$g^{\Delta_1}_{\pi \Delta_p}$	0.5300	$g^{\Delta_2}_{\pi \Delta_p}$	0.2289
$g^{\Delta_1}_{\pi \Delta_f}$	0.0004	$g^{\Delta_2}_{\pi \Delta_f}$	0.0075
$\Lambda^{\Delta_1}_{\pi N}/\text{GeV}$	0.8246	$\Lambda^{\Delta_2}_{\pi N}/\text{GeV}$	1.3384
$\Lambda^{\Delta_1}_{\pi \Delta_p}/\text{GeV}$	0.8376	$\Lambda^{\Delta_2}_{\pi \Delta_p}/\text{GeV}$	0.5428
$\Lambda^{\Delta_1}_{\pi \Delta_f}/\text{GeV}$	0.5776	$\Lambda^{\Delta_2}_{\pi \Delta_f}/\text{GeV}$	1.0549
$v_{\pi N, \pi N}$	0.0454	$v_{\pi N, \pi \Delta_f}$	-0.0030
$v_{\pi N, \pi \Delta_p}$	-1.5545	$v_{\pi \Delta_p, \pi \Delta_f}$	-0.0053
$v_{\pi \Delta_p, \pi \Delta_p}$	-0.9694	$v_{\pi \Delta_f, \pi \Delta_f}$	-0.0001
$\Lambda^{v}_{\pi N}/\text{GeV}$	0.6032	$\Lambda^{v}_{\pi \Delta_f}/\text{GeV}$	1.3289
$\Lambda^{v}_{\pi \Delta_p}/\text{GeV}$	0.8058		

Bare Slope (GeV^{-1})	Value
α_{Δ_1}	0.751
α_{Δ_2}	0.203

Section 3

$\Delta\frac{3}{2}^{+}$ State Composition

Δ Finite Volume Spectrum at $L = 3$ fm

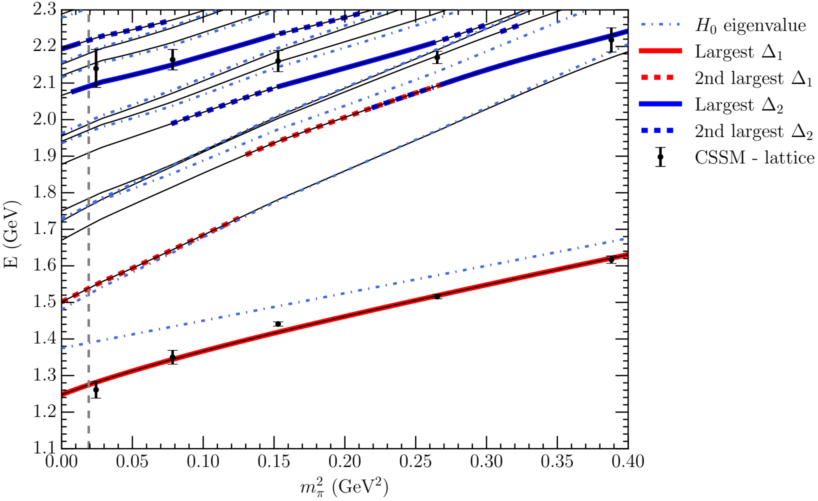

Eigenstate Composition: State 1 – Δ_1 dominated

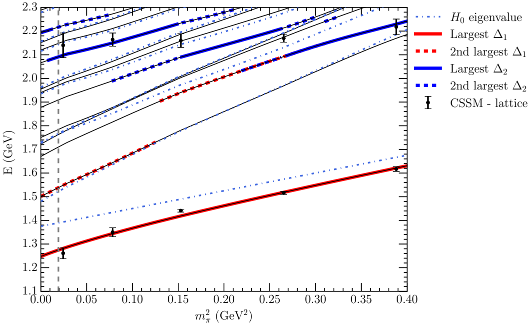

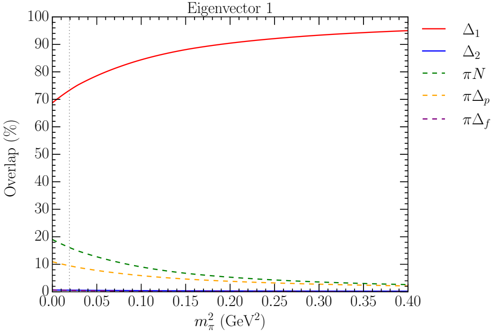

Eigenstate Composition: State 2 – πN dominated

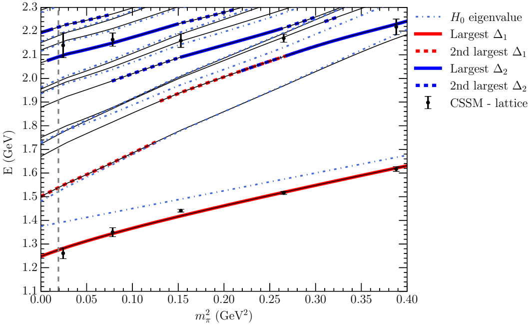

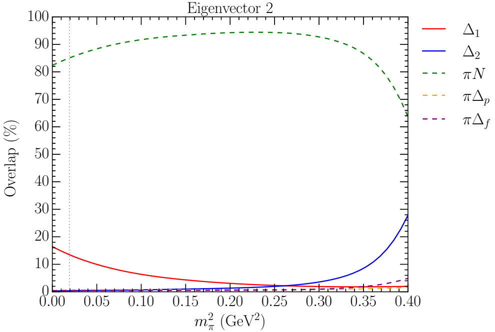

Eigenstate Composition: State 3 – Mix of 3 two-particle channels

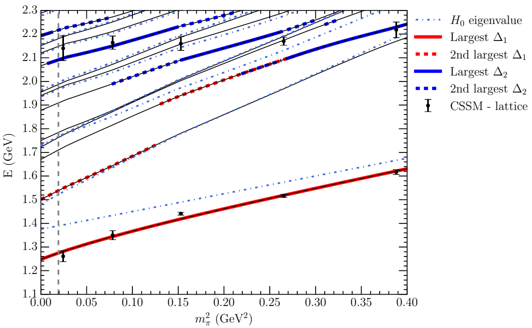

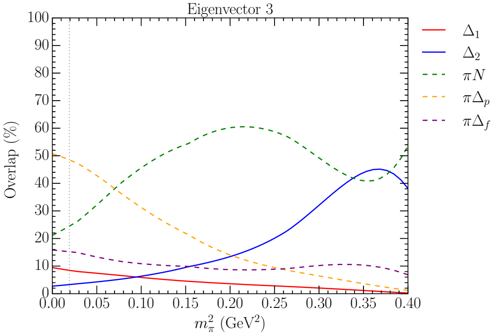

Eigenstate Composition: State 4 – $\pi\Delta_f$ dominated

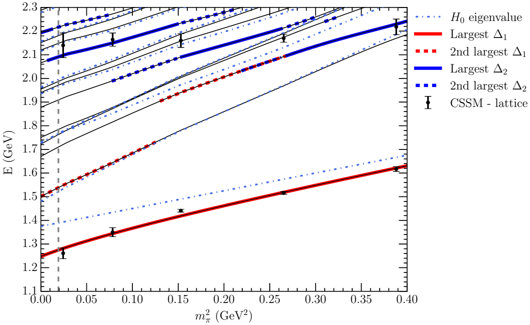

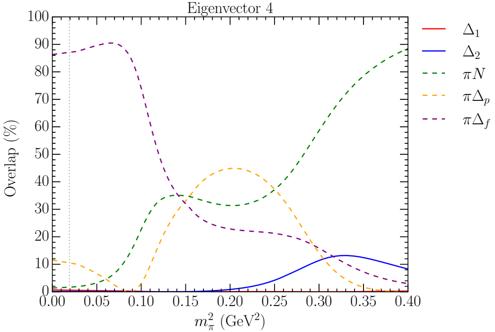

Eigenstate Composition: State 5 – Mix of πN and $\pi\Delta_p$

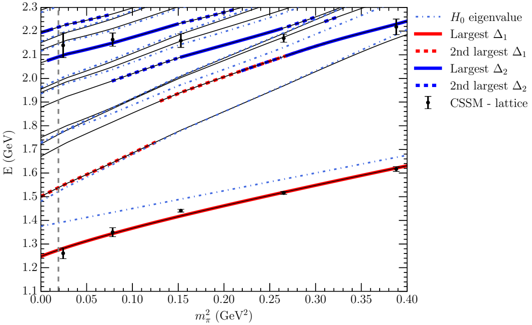

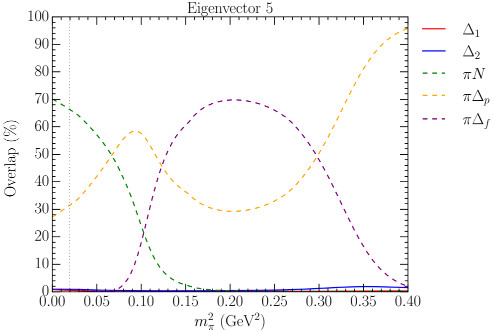

Eigenstate Composition: State 6 – Mix of 3 channels and Δ_2

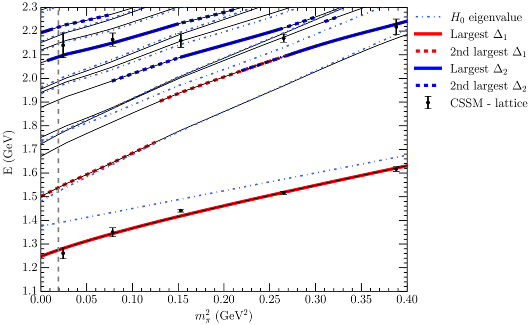

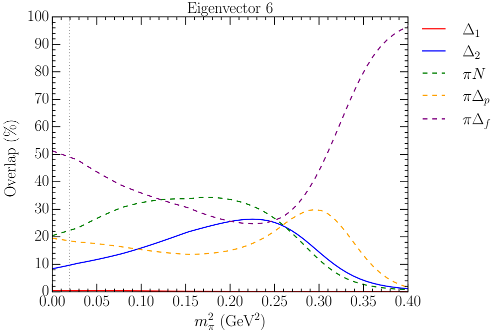

Eigenstate Composition: State 7 – πN dominated

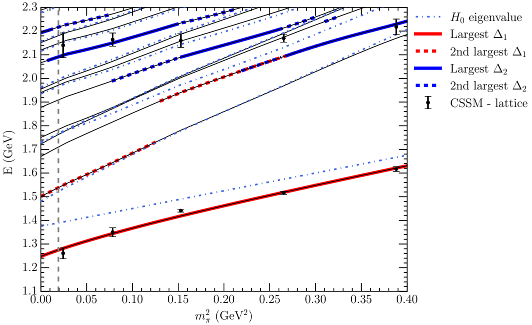

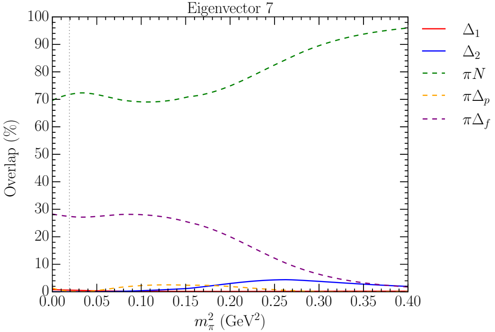

Eigenstate Composition: State 8 – $\pi\Delta_p$ dominated

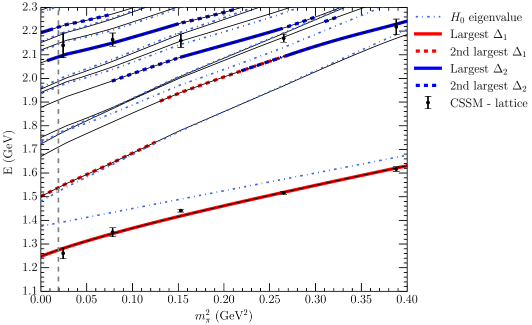

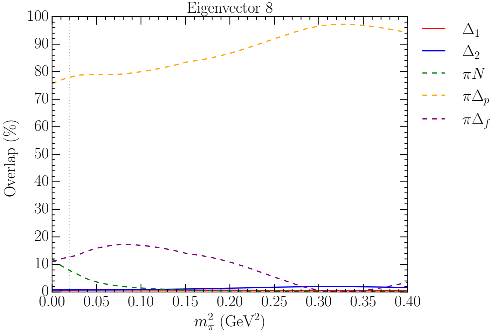

Eigenstate Composition: State 9 – Largest Δ_2 component

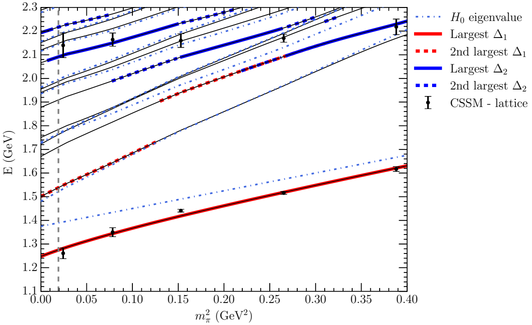

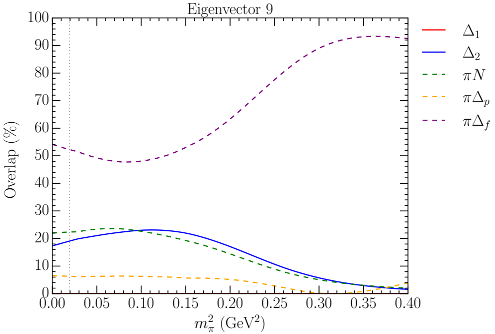

Comparison with other Lattice Collaborations

- CLS Consortium:

  C. Morningstar, J. Bulava, A. D. Hanlon, B. Hörz, D. Mohler, A. Nicholson, S. Skinner and A. Walker-Loud, PoS **LATTICE2021** (2022), 170 [arXiv:2111.07755 [hep-lat]].

Comparison with other Lattice Collaborations

- CLS Consortium:
  C. Morningstar, J. Bulava, A. D. Hanlon, B. Hörz, D. Mohler, A. Nicholson, S. Skinner and A. Walker-Loud, PoS **LATTICE2021** (2022), 170 [arXiv:2111.07755 [hep-lat]].

- Cyprus Collaboration:
  C. Alexandrou, S. Bacchio, G. Koutsou, T. Leontiou, S. Paul, M. Petschlies and F. Pittler, Phys. Rev. D **109** (2024) no.3, 3 [arXiv:2307.12846 [hep-lat]].

Comparison with other Lattice Collaborations

- CLS Consortium:
  C. Morningstar, J. Bulava, A. D. Hanlon, B. Hörz, D. Mohler, A. Nicholson, S. Skinner and A. Walker-Loud, PoS **LATTICE2021** (2022), 170 [arXiv:2111.07755 [hep-lat]].

- Cyprus Collaboration:
  C. Alexandrou, S. Bacchio, G. Koutsou, T. Leontiou, S. Paul, M. Petschlies and F. Pittler, Phys. Rev. D **109** (2024) no.3, 3 [arXiv:2307.12846 [hep-lat]].

- Hadron Spectrum Collaboration (HSC):
  J. Bulava, R. G. Edwards, E. Engelson, B. Joo, H. W. Lin, C. Morningstar, D. G. Richards and S. J. Wallace, Phys. Rev. D **82** (2010), 014507 [arXiv:1004.5072 [hep-lat]].

Comparison with other Lattice Collaborations

- CLS Consortium:
  C. Morningstar, J. Bulava, A. D. Hanlon, B. Hörz, D. Mohler, A. Nicholson, S. Skinner and A. Walker-Loud, PoS **LATTICE2021** (2022), 170 [arXiv:2111.07755 [hep-lat]].

- Cyprus Collaboration:
  C. Alexandrou, S. Bacchio, G. Koutsou, T. Leontiou, S. Paul, M. Petschlies and F. Pittler, Phys. Rev. D **109** (2024) no.3, 3 [arXiv:2307.12846 [hep-lat]].

- Hadron Spectrum Collaboration (HSC):
  J. Bulava, R. G. Edwards, E. Engelson, B. Joo, H. W. Lin, C. Morningstar, D. G. Richards and S. J. Wallace, Phys. Rev. D **82** (2010), 014507 [arXiv:1004.5072 [hep-lat]].

- Khan, *et al.*:
  T. Khan, D. Richards and F. Winter, Phys. Rev. D **104** (2021) no.3, 034503 [arXiv:2010.03052 [hep-lat]].

CLS Consortium Spectrum at $L = 4.16$ fm from 2022

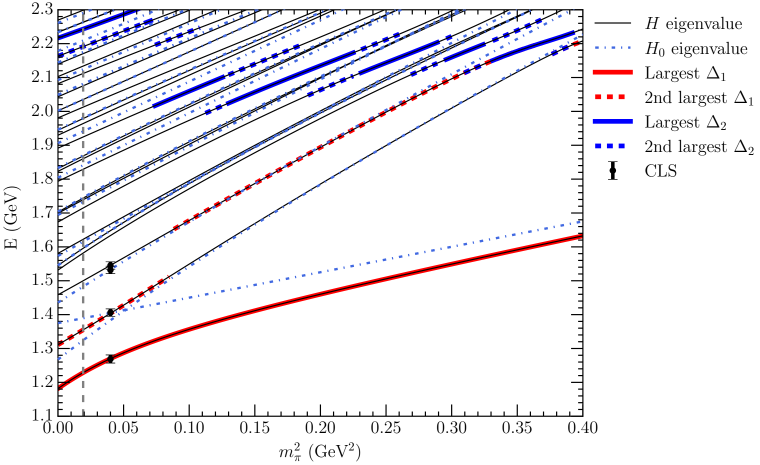

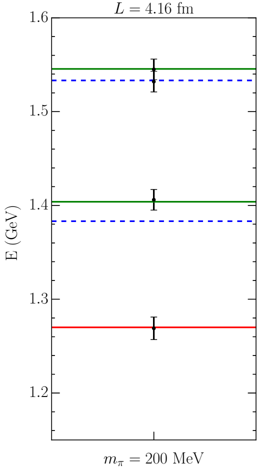

Eigenstate Composition: State 1 – Δ_1 dominated

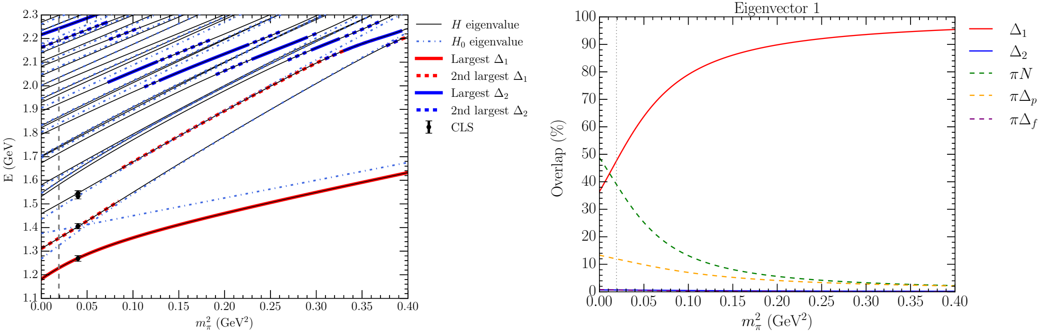

Eigenstate Composition: State 2 – πN dominated

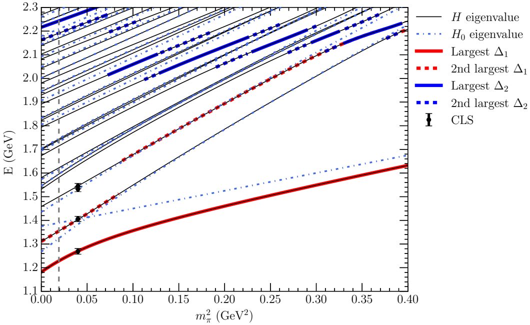

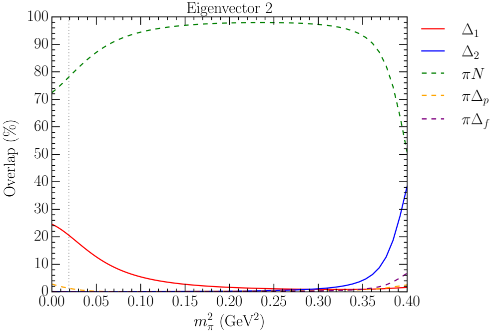

Eigenstate Composition: State 3 – Also πN dominated

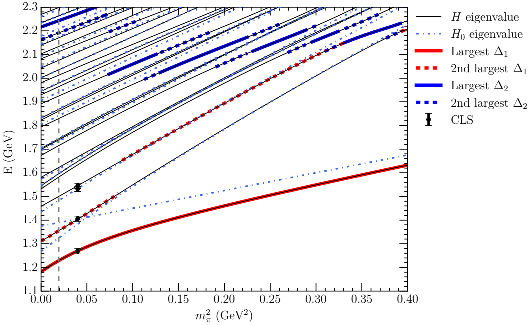

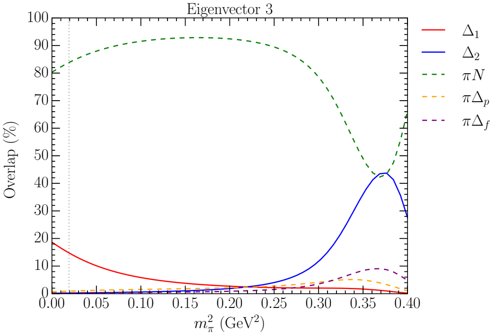

Cyprus Collaboration: $m_\pi = 0.139$ GeV and $L = 5.1$ fm from 2024

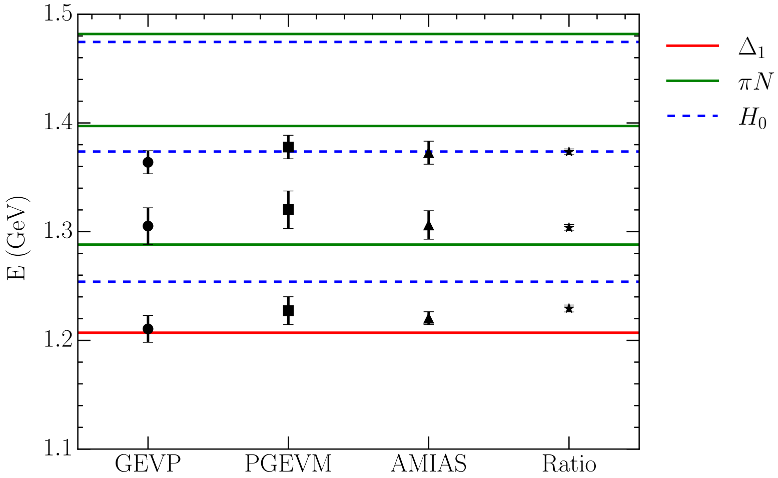

HSC Spectrum at $L = 1.96$ fm from 2010

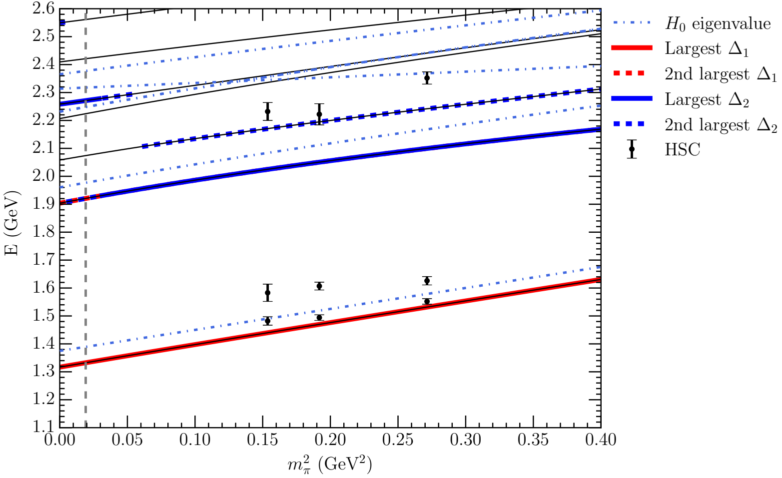

Khan *et al.* Spectrum at $L = 3.01$ fm from 2021

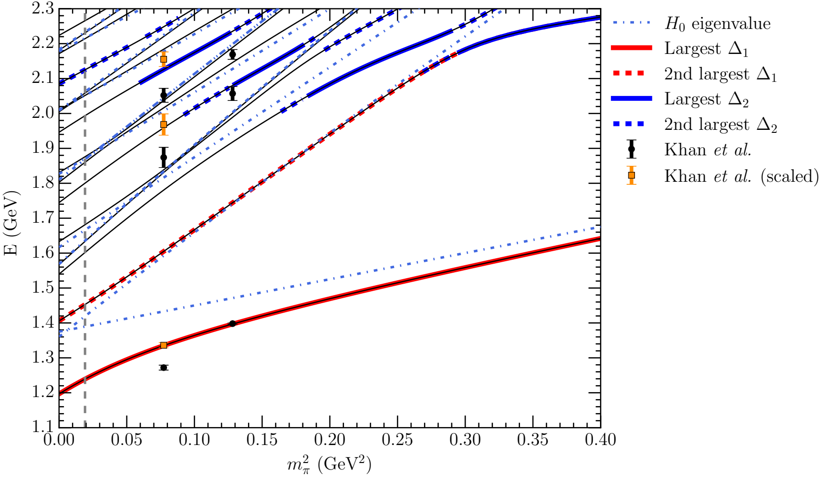

Section 4

$\Lambda\frac{1}{2}^-$ Analysis

New analysis of low-lying odd-parity Λ resonances

J. J. Liu, Z. W. Liu, K. Chen, D. Guo, DBL, X. Liu and A. W. Thomas,
Phys. Rev. D **109** (2024) 054025 [arXiv:2312.13072 [hep-ph]]

New analysis of low-lying odd-parity Λ resonances

J. J. Liu, Z. W. Liu, K. Chen, D. Guo, DBL, X. Liu and A. W. Thomas,
Phys. Rev. D **109** (2024) 054025 [arXiv:2312.13072 [hep-ph]]

- Motivated by recent advances in both experiment and theory.

New analysis of low-lying odd-parity Λ resonances

J. J. Liu, Z. W. Liu, K. Chen, D. Guo, DBL, X. Liu and A. W. Thomas,
Phys. Rev. D **109** (2024) 054025 [arXiv:2312.13072 [hep-ph]]

- Motivated by recent advances in both experiment and theory.

- Considerable progress in new K^-p scattering data associated with $\Lambda\frac{1}{2}^-$ baryons.
  - 2022: DAΦNE: Near threshold cross section measurements.
  - 2022: J-PARC: $\pi\Sigma$ invariant mass spectra in K^-p induced reactions.
  - 2021: ALICE: K^-p scattering length.

New analysis of low-lying odd-parity Λ resonances

J. J. Liu, Z. W. Liu, K. Chen, D. Guo, DBL, X. Liu and A. W. Thomas,
Phys. Rev. D **109** (2024) 054025 [arXiv:2312.13072 [hep-ph]]

- Motivated by recent advances in both experiment and theory.

- Considerable progress in new K^-p scattering data associated with $\Lambda\frac{1}{2}^-$ baryons.
  - 2022: DAΦNE: Near threshold cross section measurements.
  - 2022: J-PARC: $\pi\Sigma$ invariant mass spectra in K^-p induced reactions.
  - 2021: ALICE: K^-p scattering length.

- BaSc Lattice QCD collaboration performed coupled-channel simulations with both single baryon and meson-baryon interpolating operators at $m_\pi = 204$ MeV.

New analysis of low-lying odd-parity Λ resonances

J. J. Liu, Z. W. Liu, K. Chen, D. Guo, DBL, X. Liu and A. W. Thomas,
Phys. Rev. D **109** (2024) 054025 [arXiv:2312.13072 [hep-ph]]

- Motivated by recent advances in both experiment and theory.
- Considerable progress in new K^-p scattering data associated with $\Lambda\frac{1}{2}^-$ baryons.
  - 2022: DAΦNE: Near threshold cross section measurements.
  - 2022: J-PARC: $\pi\Sigma$ invariant mass spectra in K^-p induced reactions.
  - 2021: ALICE: K^-p scattering length.
- BaSc Lattice QCD collaboration performed coupled-channel simulations with both single baryon and meson-baryon interpolating operators at $m_\pi = 204$ MeV.
- Extend the analysis of the cross section data for K^-p scattering to K^- laboratory momenta of 800 MeV/c to address the $\Lambda(1670)$.

Analysis of low-lying odd-parity Λ resonances

J. J. Liu, Z. W. Liu, K. Chen, D. Guo, D.B.L., X. Liu and A. W. Thomas,
Phys. Rev. D **109** (2024) 054025 [arXiv:2312.13072 [hep-ph]]

- Consider $\pi\Sigma$, $\bar{K}N$, $\eta\Lambda$, $K\Xi$ channels, and one bare basis state, B_0.
  - The mass of $\Lambda(1670)$ is only 130 MeV below the $K\Xi$ threshold.

Analysis of low-lying odd-parity Λ resonances

J. J. Liu, Z. W. Liu, K. Chen, D. Guo, D.B.L., X. Liu and A. W. Thomas,
Phys. Rev. D **109** (2024) 054025 [arXiv:2312.13072 [hep-ph]]

- Consider $\pi\Sigma$, $\bar{K}N$, $\eta\Lambda$, $K\Xi$ channels, and one bare basis state, B_0.
  - The mass of $\Lambda(1670)$ is only 130 MeV below the $K\Xi$ threshold.

- 16 two-to-two particle couplings are considered in isospin 0 and 1.

Analysis of low-lying odd-parity Λ resonances

J. J. Liu, Z. W. Liu, K. Chen, D. Guo, D.B.L., X. Liu and A. W. Thomas,
Phys. Rev. D **109** (2024) 054025 [arXiv:2312.13072 [hep-ph]]

- Consider $\pi\Sigma$, $\bar{K}N$, $\eta\Lambda$, $K\Xi$ channels, and one bare basis state, B_0.
  - The mass of $\Lambda(1670)$ is only 130 MeV below the $K\Xi$ threshold.
- 16 two-to-two particle couplings are considered in isospin 0 and 1.
- Five parameters describe the bare to two-particle interactions

$$g^0_{B_0,\pi\Sigma} \quad g^0_{B_0,\bar{K}N} \quad g^0_{B_0,\eta\Lambda} \quad g^0_{B_0,K\Xi} \quad m_{B_0}$$

Analysis of low-lying odd-parity Λ resonances

J. J. Liu, Z. W. Liu, K. Chen, D. Guo, D.B.L., X. Liu and A. W. Thomas,
Phys. Rev. D **109** (2024) 054025 [arXiv:2312.13072 [hep-ph]]

- Consider $\pi\Sigma$, $\bar{K}N$, $\eta\Lambda$, $K\Xi$ channels, and one bare basis state, B_0.
  - The mass of $\Lambda(1670)$ is only 130 MeV below the $K\Xi$ threshold.

- 16 two-to-two particle couplings are considered in isospin 0 and 1.

- Five parameters describe the bare to two-particle interactions

$$g^0_{B_0,\pi\Sigma} \quad g^0_{B_0,\bar{K}N} \quad g^0_{B_0,\eta\Lambda} \quad g^0_{B_0,K\Xi} \quad m_{B_0}$$

- No new parameters in going to the finite volume of the lattice.
  - The bare mass slope is taken to be $\frac{2}{3}$ of our previous $N\frac{1}{2}^-(1535)$ analysis slope.

Fits to experimental cross-section data σ/mb vs $|\vec{p}_{\text{lab}}|/\text{MeV}$

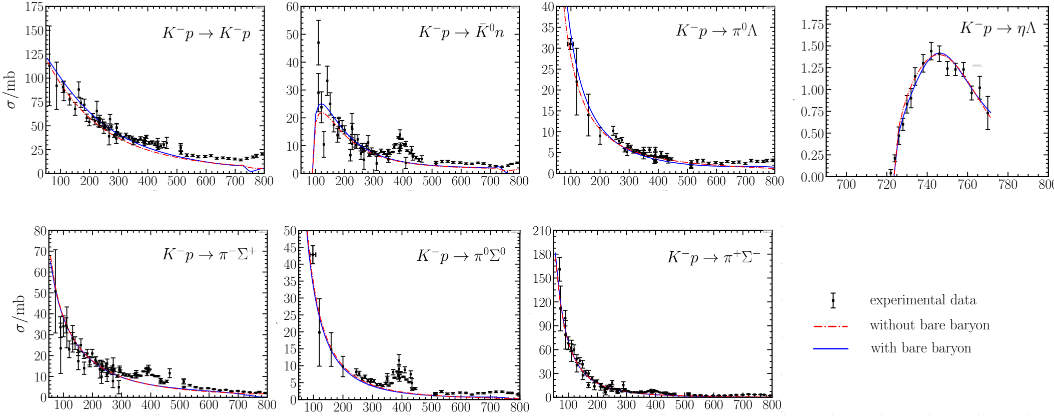

- Note the presence of two fits, one with and one without a single-particle basis state.

Fits to experimental cross-section data σ/mb vs $|\vec{p}_{\mathrm{lab}}|/\mathrm{MeV}$

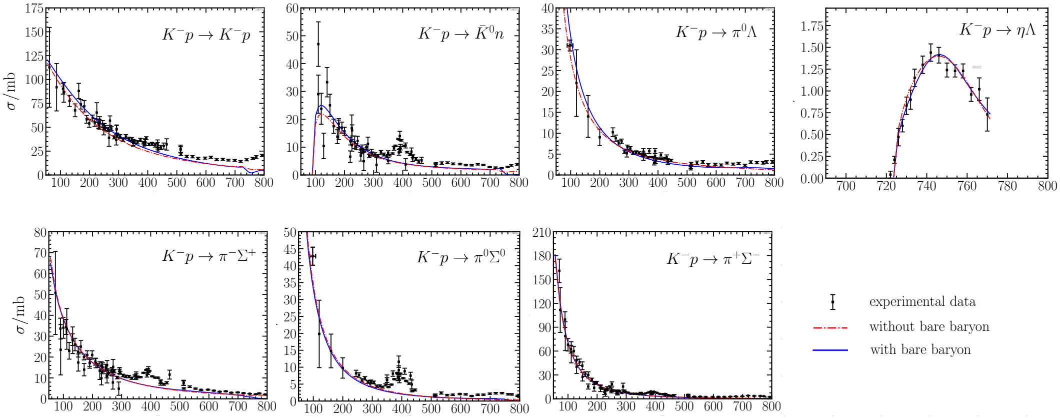

- The peak of $\Lambda(1670)$ can be clearly seen in the $K^-p \to \eta\Lambda$ channel.

Fits to experimental cross-section data σ/mb vs $|\vec{p}_{\text{lab}}|/\text{MeV}$

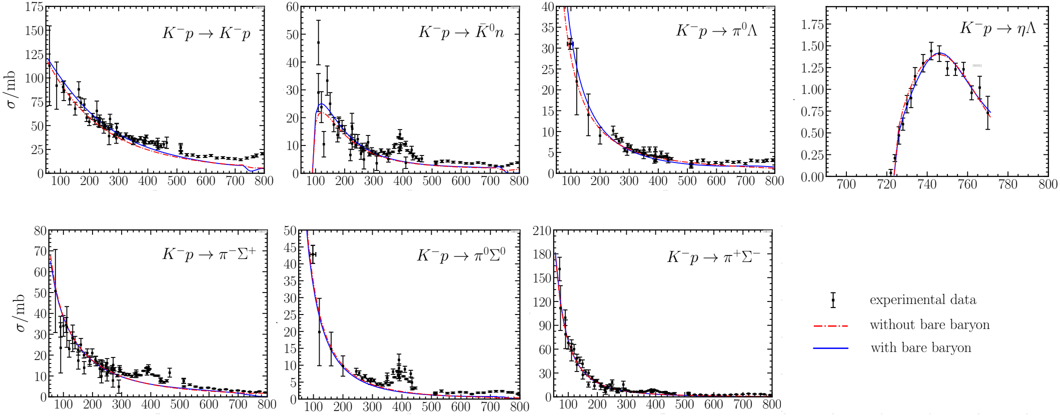

- The peaks around 400 MeV are associated with the D-wave $\Lambda(1520)$ state.

Fits to experimental cross-section data σ/mb vs $|\vec{p}_{\text{lab}}|/\text{MeV}$

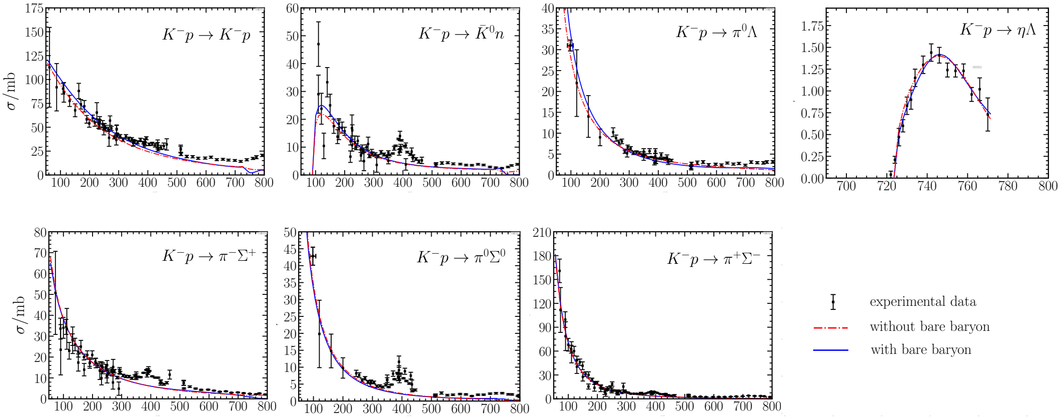

- $\bar{K}^*N$ and $\pi\Sigma^*$ channels (not included) will contribute at large $|\vec{p}_{\text{lab}}| > 500$ MeV.

Fits to experimental cross-section data σ/mb vs $|\vec{p}_{\text{lab}}|/\text{MeV}$

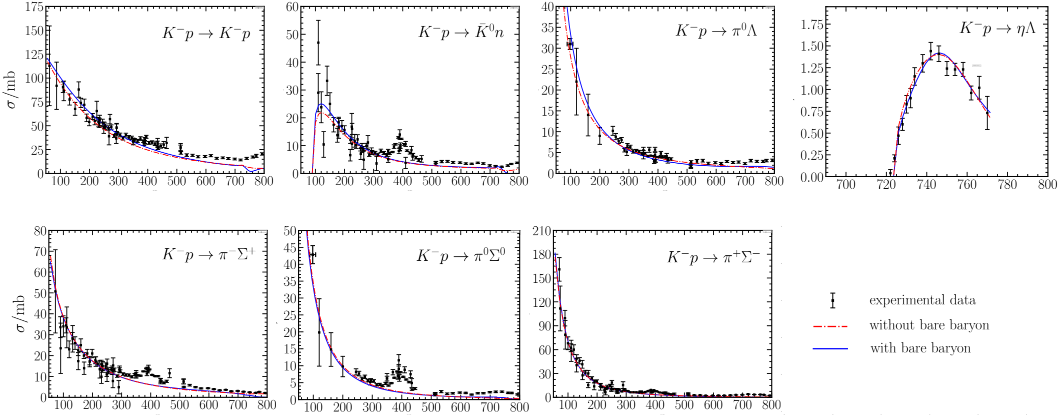

- The three poles generated by these fits are very similar.

Fits to experimental cross-section data σ/mb vs $|\vec{p}_{\text{lab}}|/\text{MeV}$

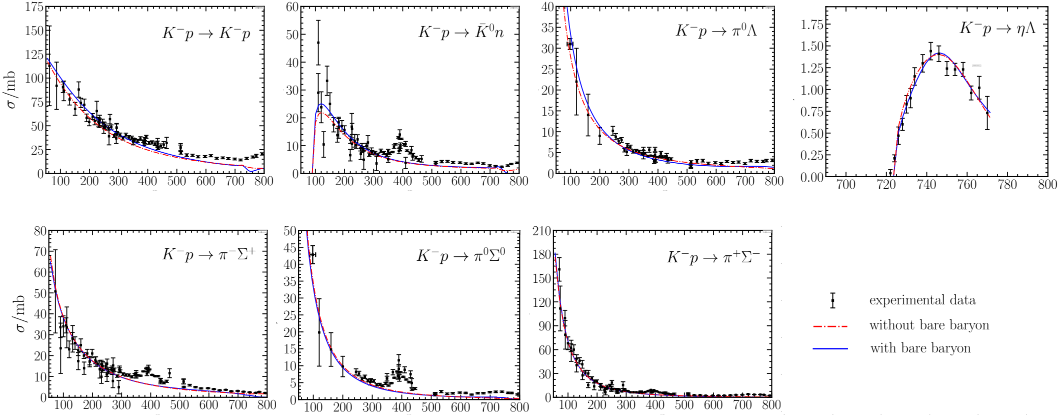

- Present experimental data are not able to distinguish between these fits.

Finite Volume Λ Spectrum for $L \simeq 3$ fm

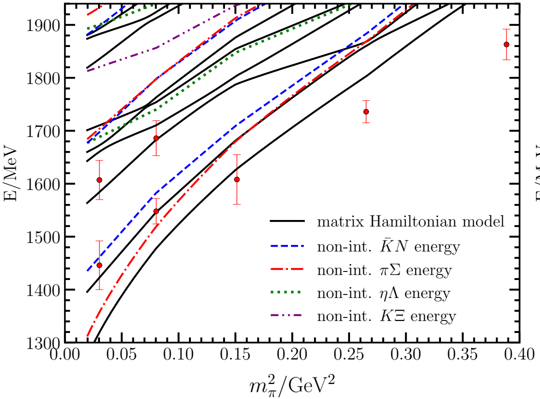

Without a bare Λ basis state.

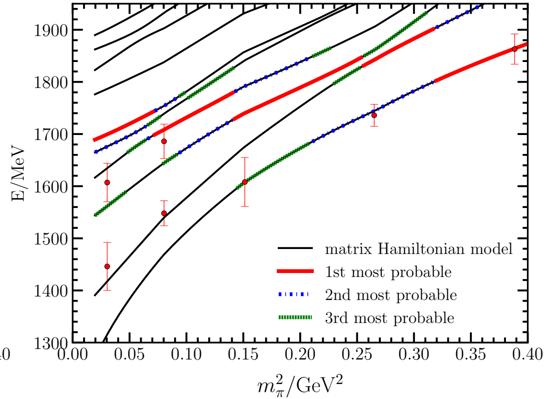

With a bare Λ basis state.

Coupling	No $\vert B_0\rangle$	With $\vert B_0\rangle$
Λ (GeV)	1.000	1.000
$g^0_{\bar{K}N,\bar{K}N}$	-2.108	-2.180
$g^0_{\bar{K}N,\pi\Sigma}$	0.837	0.620
$g^0_{\bar{K}N,\eta\Lambda}$	-0.461	-0.472
$g^0_{\pi\Sigma,\pi\Sigma}$	-1.728	-1.200
$g^0_{\pi\Sigma,K\Xi}$	-0.001	-1.800
$g^0_{\eta\Lambda,K\Xi}$	0.835	1.993
$g^0_{K\Xi,K\Xi}$	-3.393	-1.000
$g^1_{\bar{K}N,\bar{K}N}$	-0.028	-0.001
$g^1_{\bar{K}N,\pi\Sigma}$	0.829	0.985
$g^1_{\bar{K}N,\pi\Lambda}$	0.001	0.990
$g^1_{\bar{K}N,\eta\Sigma}$	1.557	1.500
$g^1_{\pi\Sigma,\pi\Sigma}$	-1.351	-0.001
$g^1_{\pi\Sigma,K\Xi}$	-1.017	-1.341
$g^1_{\pi\Lambda,K\Xi}$	2.904	0.011
$g^1_{\eta\Sigma,K\Xi}$	4.690	0.001
$g^1_{K\Xi,K\Xi}$	-0.447	-3.700

21 Fit Parameters

Coupling	No $\vert B_0\rangle$	With $\vert B_0\rangle$
$g^0_{B_0,\bar{K}N}$	–	0.091
$g^0_{B_0,\pi\Sigma}$	–	0.049
$g^0_{B_0,\eta\Lambda}$	–	-0.164
$g^0_{B_0,K\Xi}$	–	-0.226
m^0_B (MeV)	–	1750
Pole 1 (MeV)	$1336 - 87\,i$	$1324 - 67\,i$
Pole 2 (MeV)	$1430 - 26\,i$	$1428 - 24\,i$
Pole 3 (MeV)	$1676 - 17\,i$	$1674 - 11\,i$

Finite Volume Λ Spectrum for $L \simeq 3$ fm

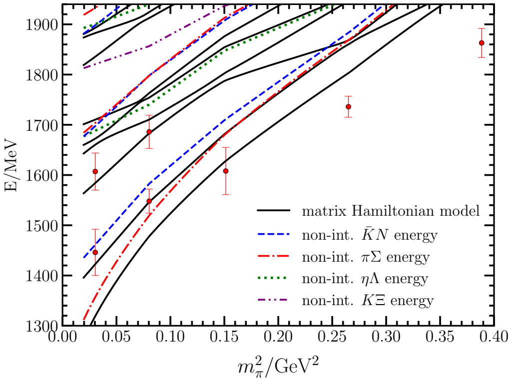

Without a bare Λ basis state.

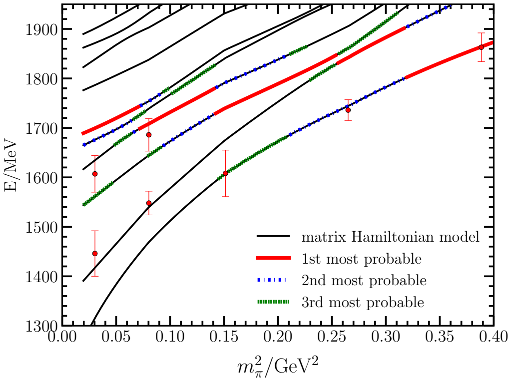

With a bare Λ basis state.

- A single-particle basis state is required to describe lattice results at large m_π^2.

Finite Volume Λ Spectrum for $L \simeq 3$ fm

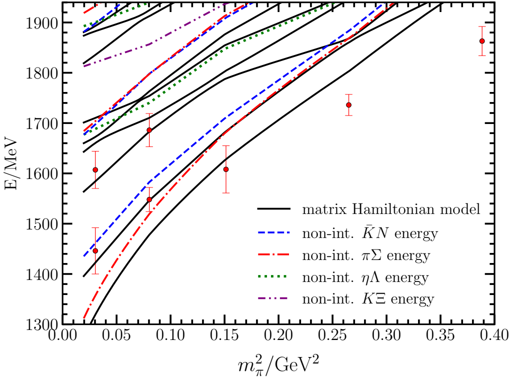

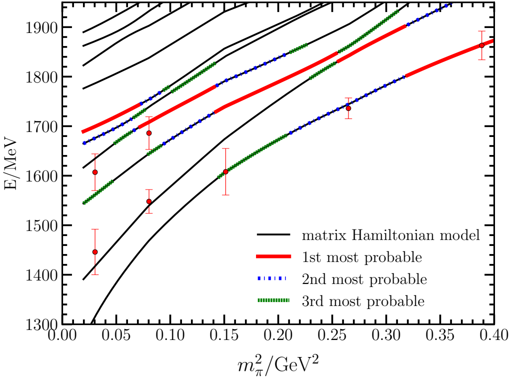

Without a bare Λ basis state. With a bare Λ basis state.

- The spectra begin to differ at the 3[rd] and 4[th] eigenstate energy.

Eigenstate Composition: $|\pi\Sigma\rangle$ dominated $\to$ $|B_0\rangle$ dominated

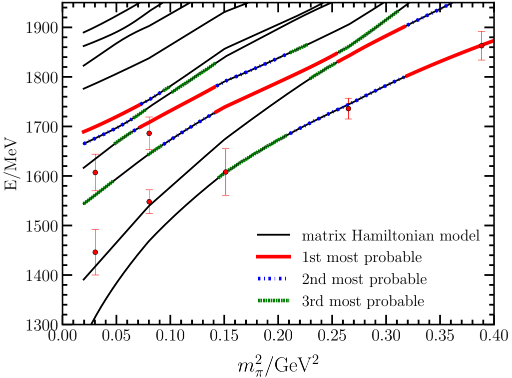

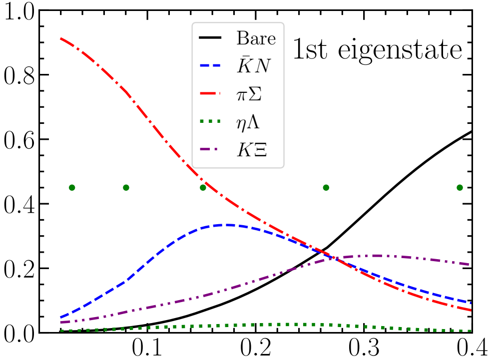

Eigenstate Composition: State 2 – $|\bar{K}N\rangle \to |\pi\Sigma\rangle \to |B_0\rangle$

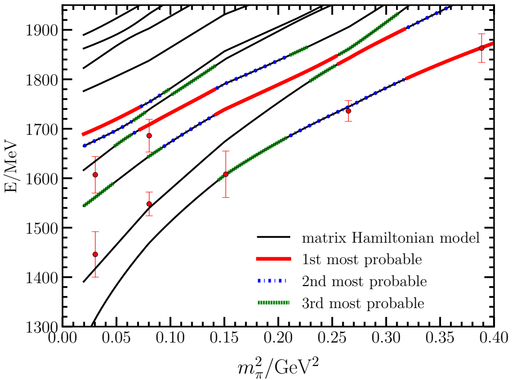

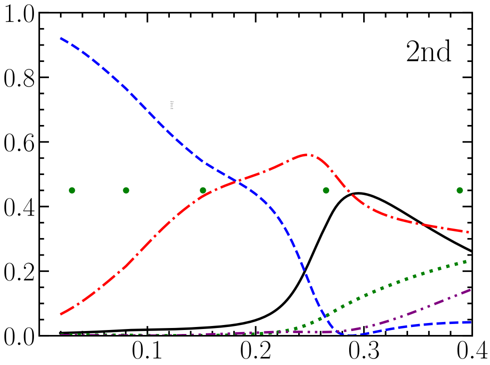

Eigenstate Composition: State 3 – First significant $|B_0\rangle$

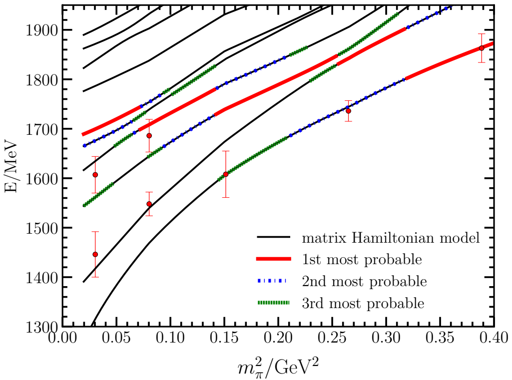

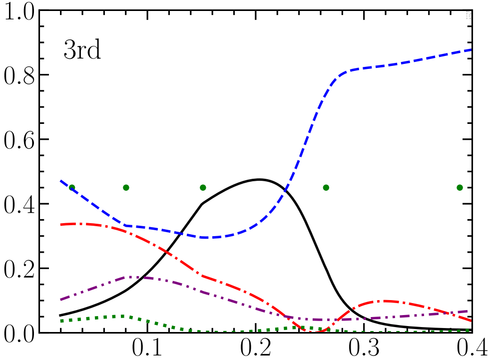

Eigenstate Composition: State 4 – $|\bar{K}N\rangle$ and $|\pi\Sigma\rangle$

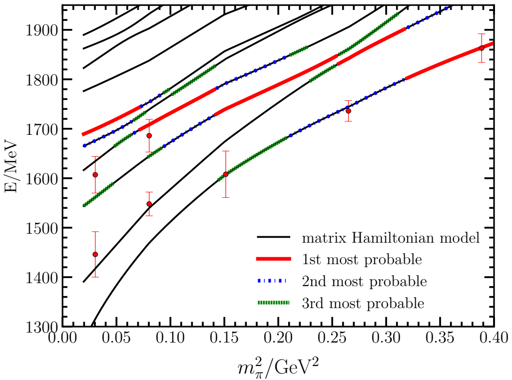

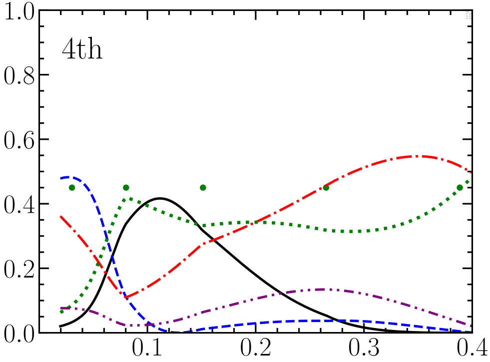

Eigenstate Composition: State 5 – $|\eta\Lambda\rangle$ and $|B_0\rangle$

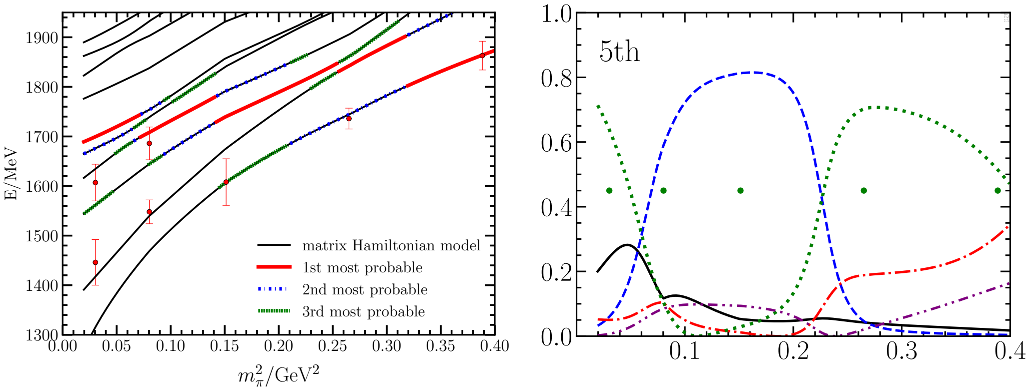

Eigenstate Composition: State 6 – $|B_0\rangle$ dominated at ~ 1670 MeV

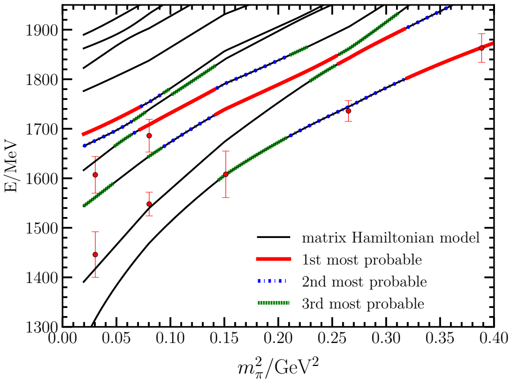

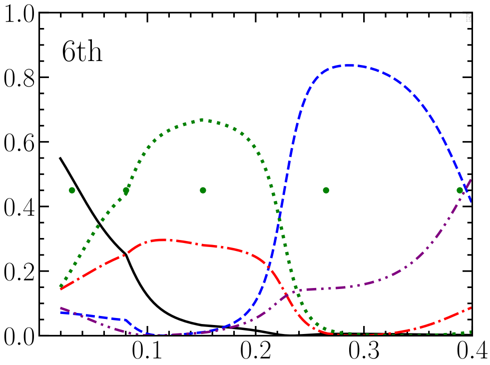

Baryon Scattering (BaSc) Collaboration Spectrum Comparison

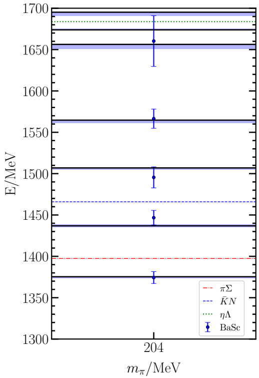

- $L = 4.05$ fm lattice at $m_\pi = 204\,$MeV.

J. Bulava *et al.* [Baryon Scattering (BaSc)], Phys. Rev. Lett. **132** (2024) 051901 [arXiv:2307.10413 [hep-lat]]
J. Bulava *et al.* [Baryon Scattering (BaSc)], Phys. Rev. D **109** (2024) 014511 [arXiv:2307.13471 [hep-lat]]

Baryon Scattering (BaSc) Collaboration Spectrum Comparison

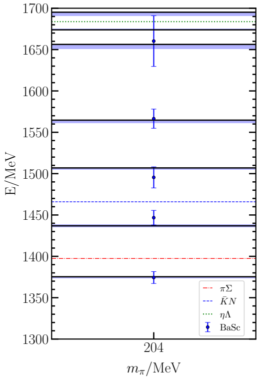

- $L = 4.05$ fm lattice at $m_\pi = 204$ MeV.
- Lattice energies from the $G_{1u}(0)$ irreducible representation.

J. Bulava *et al.* [Baryon Scattering (BaSc)], Phys. Rev. Lett. **132** (2024) 051901 [arXiv:2307.10413 [hep-lat]]
J. Bulava *et al.* [Baryon Scattering (BaSc)], Phys. Rev. D **109** (2024) 014511 [arXiv:2307.13471 [hep-lat]]

Baryon Scattering (BaSc) Collaboration Spectrum Comparison

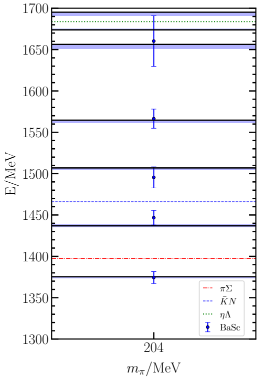

- $L = 4.05$ fm lattice at $m_\pi = 204$ MeV.
- Lattice energies from the $G_{1u}(0)$ irreducible representation.
- Solid lines are HEFT predictions.

J. Bulava *et al.* [Baryon Scattering (BaSc)], Phys. Rev. Lett. **132** (2024) 051901 [arXiv:2307.10413 [hep-lat]]

J. Bulava *et al.* [Baryon Scattering (BaSc)], Phys. Rev. D **109** (2024) 014511 [arXiv:2307.13471 [hep-lat]]

Baryon Scattering (BaSc) Collaboration Spectrum Comparison

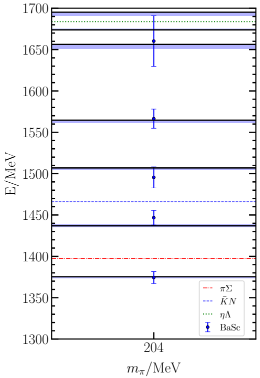

- $L = 4.05$ fm lattice at $m_\pi = 204$ MeV.
- Lattice energies from the $G_{1u}(0)$ irreducible representation.
- Solid lines are HEFT predictions.
- Blue highlights illustrate the uncertainty allowed by expt.

J. Bulava *et al.* [Baryon Scattering (BaSc)], Phys. Rev. Lett. **132** (2024) 051901 [arXiv:2307.10413 [hep-lat]]
J. Bulava *et al.* [Baryon Scattering (BaSc)], Phys. Rev. D **109** (2024) 014511 [arXiv:2307.13471 [hep-lat]]

Baryon Scattering (BaSc) Collaboration Spectrum Comparison

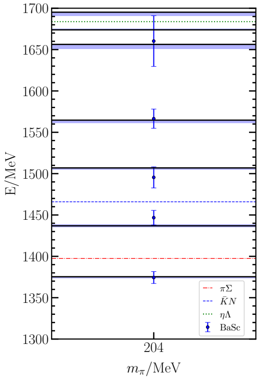

- $L = 4.05$ fm lattice at $m_\pi = 204\,$MeV.
- Lattice energies from the $G_{1u}(0)$ irreducible representation.
- Solid lines are HEFT predictions.
- Blue highlights illustrate the uncertainty allowed by expt.
- Dashed lines indicate the non-interacting threshold energies for $\pi\Sigma$ and $\bar{K}N$.

J. Bulava *et al.* [Baryon Scattering (BaSc)], Phys. Rev. Lett. **132** (2024) 051901 [arXiv:2307.10413 [hep-lat]]

J. Bulava *et al.* [Baryon Scattering (BaSc)], Phys. Rev. D **109** (2024) 014511 [arXiv:2307.13471 [hep-lat]]

Baryon Scattering (BaSc) Collaboration Spectrum Comparison

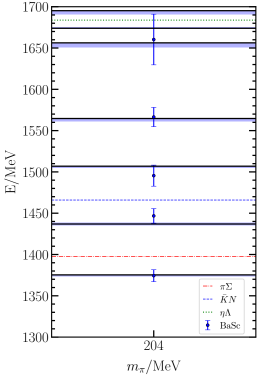

- $L = 4.05$ fm lattice at $m_\pi = 204\,$MeV.
- Lattice energies from the $G_{1u}(0)$ irreducible representation.
- Solid lines are HEFT predictions.
- Blue highlights illustrate the uncertainty allowed by expt.
- Dashed lines indicate the non-interacting threshold energies for $\pi\Sigma$ and $\bar{K}N$.
- All states are observed, and agree within 1σ.

J. Bulava *et al.* [Baryon Scattering (BaSc)], Phys. Rev. Lett. **132** (2024) 051901 [arXiv:2307.10413 [hep-lat]]
J. Bulava *et al.* [Baryon Scattering (BaSc)], Phys. Rev. D **109** (2024) 014511 [arXiv:2307.13471 [hep-lat]]

Baryon Scattering (BaSc) Collaboration Spectrum Comparison

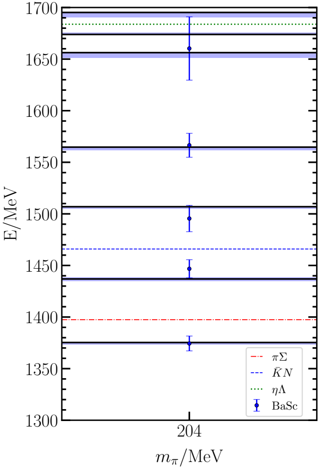

Basis includes $|B_0\rangle$

Baryon Scattering (BaSc) Collaboration Spectrum Comparison

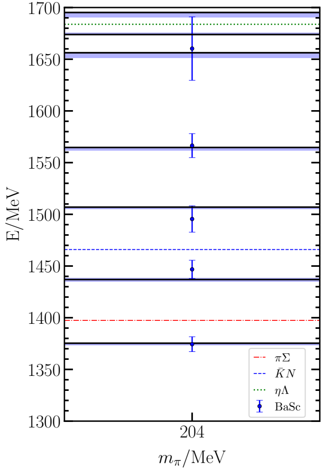

Basis includes $|B_0\rangle$

- Recall the 3rd and 4th HEFT energies are sensitive to $|B_0\rangle$.

Baryon Scattering (BaSc) Collaboration Spectrum Comparison

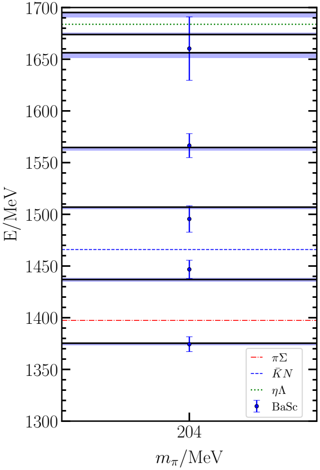

Basis includes $|B_0\rangle$

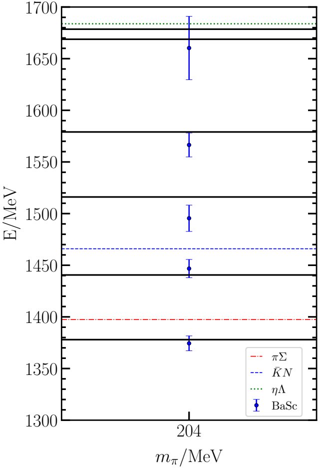

No $|B_0\rangle$

- Recall the 3rd and 4th HEFT energies are sensitive to $|B_0\rangle$.
- Without a single-particle basis state (right), 1σ agreement is lost.

Baryon Scattering (BaSc) Collaboration Spectrum Comparison

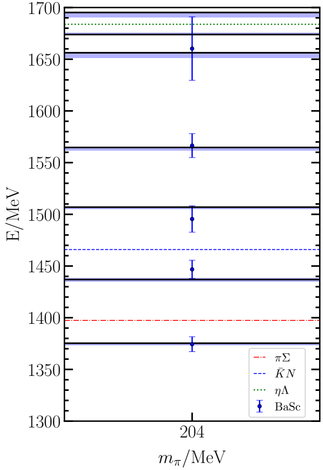

Basis includes $|B_0\rangle$

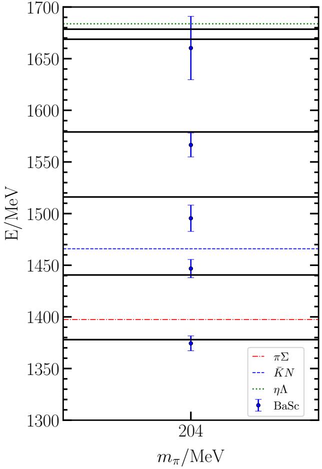

No $|B_0\rangle$

- Recall the 3rd and 4th HEFT energies are sensitive to $|B_0\rangle$.
- Without a single-particle basis state (right), 1σ agreement is lost.
- Future precision results will decide the role of $|B_0\rangle$ unambiguously.

Section 5

$N\frac{1}{2}^+$ Analysis

The $2s$ excitation of the nucleon sits at 1.9 GeV

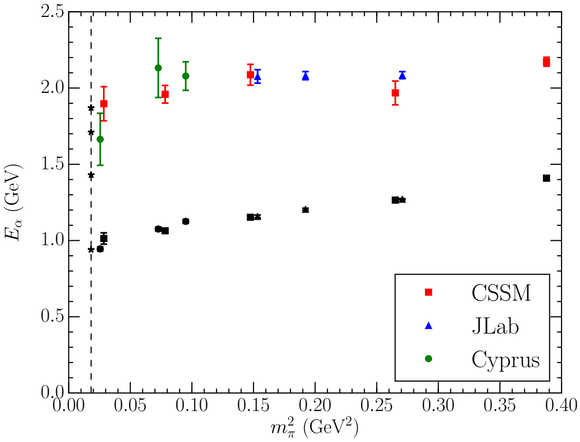

The $2s$ excitation of the nucleon sits at 1.9 GeV

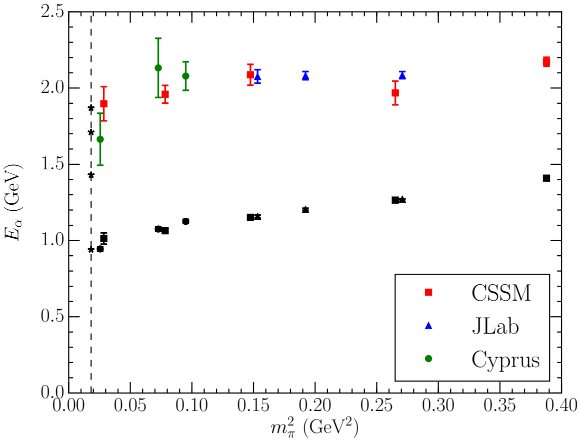

- Quark model states are basis states that mix with meson-baryon multiparticle states.

The $2s$ excitation of the nucleon sits at 1.9 GeV

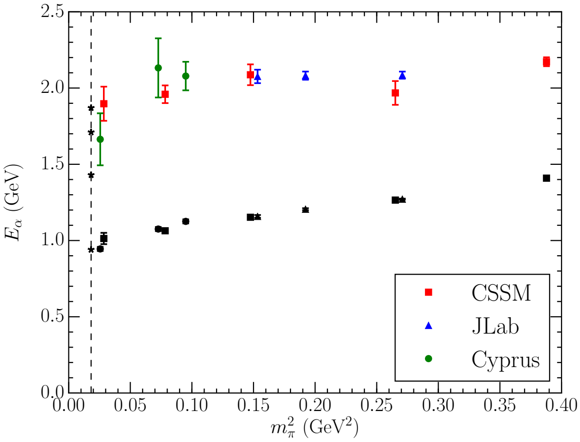

- Quark model states are basis states that mix with meson-baryon multiparticle states.
- Anticipate the $2s$ excitation is associated with
  - $N1/2^+(1880)$ observed in photoproduction.
  - $N1/2^+(1710)$ only 170 MeV away.

The $2s$ excitation of the nucleon sits at 1.9 GeV

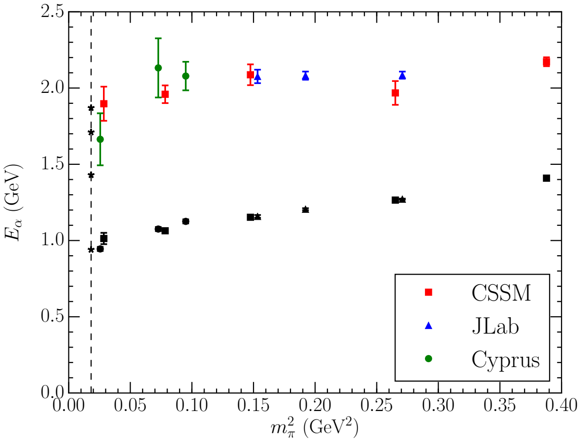

- Quark model states are basis states that mix with meson-baryon multiparticle states.
- Anticipate the $2s$ excitation is associated with
  - $N1/2^+(1880)$ observed in photoproduction.
  - $N1/2^+(1710)$ only 170 MeV away.
- What about the Roper resonance?

Positive-parity Nucleon Spectrum: Bare Basis State with $m_0 = 1.7$ GeV

J. j. Wu, DBL, Z. w. Liu and A. W. Thomas, Phys. Rev. D **97** (2018) no.9, 094509 [arXiv:1703.10715 [nucl-th]].

- Consider πN, $\pi\Delta$ and σN channels, dressing a bare basis state.
- Fit to phase shift and inelasticity. (dashed blue curve)

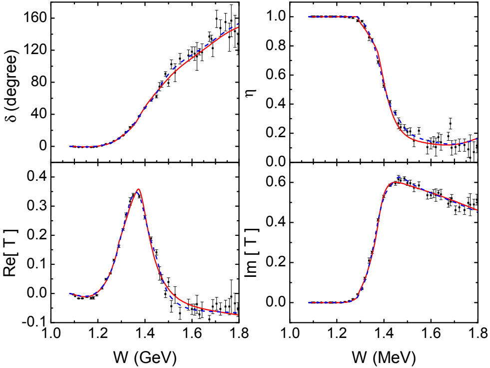

- Fit yields two poles in the region of the PDG estimate $1365 \pm 15 - i\,95 \pm 15$ MeV.

Positive-parity Nucleon Spectrum: Bare Basis State with $m_0 = 2.0$ GeV

J. j. Wu, *et al.* [CSSM], arXiv:1703.10715 [nucl-th]

- Consider πN, $\pi\Delta$ and σN channels, dressing a bare basis state.
- Fit to phase shift and inelasticity. (red curve)

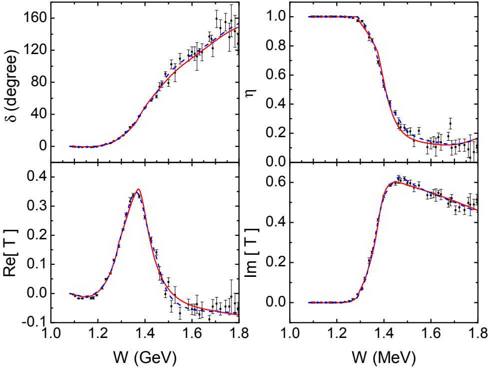

- Fit yields a pole in the regime of the PDG estimate $1365 \pm 15 - i\,95 \pm 15$ MeV.

2.0 GeV Bare Basis State: Hamiltonian Model N' Spectrum

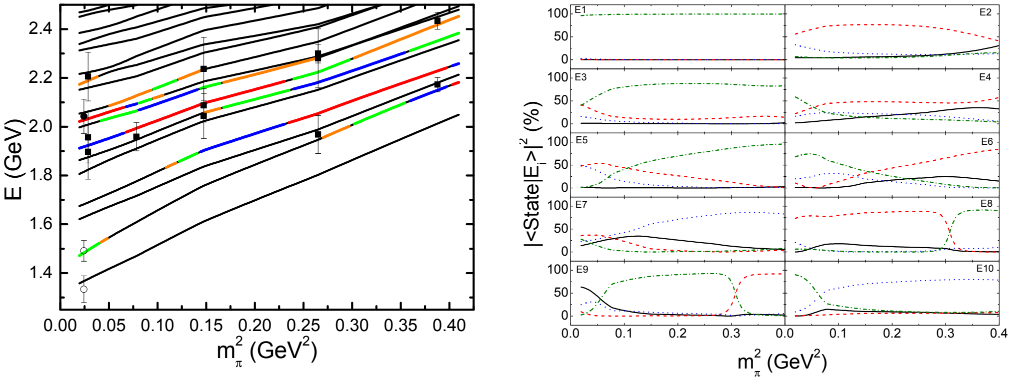

πN, $\pi\Delta$ and σN channels, dressing a bare state.

C. B. Lang, L. Leskovec, M. Padmanath and S. Prelovsek, Phys. Rev. D **95**, no. 1, 014510 (2017) [arXiv:1610.01422 [hep-lat]].

Two different descriptions of the Roper resonance

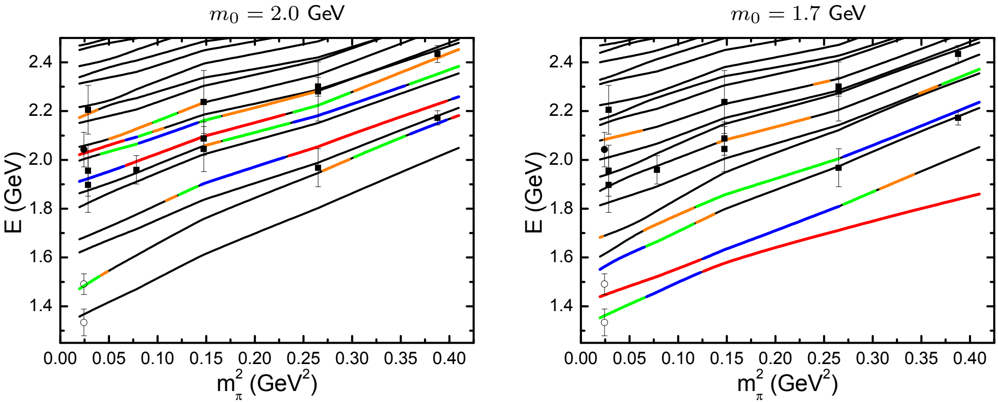

(left) Resonance generated by strong rescattering in meson-baryon channels.
(right) Meson dressings of a quark-model like core.

Section 6

Missing Baryon Resonances

Missing Baryon Resonances

- Many resonances predicted by the constituent quark model (CQM) below 2 GeV are not seen.

Missing Baryon Resonances

- Many resonances predicted by the constituent quark model (CQM) below 2 GeV are not seen.
- Now know the CQM should have been tuned to a $2s$ resonance at ~ 1900 MeV.
  - Further excitations are at energies exceeding 2 GeV.

Missing Baryon Resonances

- Many resonances predicted by the constituent quark model (CQM) below 2 GeV are not seen.
- Now know the CQM should have been tuned to a $2s$ resonance at ~ 1900 MeV.
  - Further excitations are at energies exceeding 2 GeV.
- Provides a new resolution of the missing baryon resonance problem.

Nucleon and Delta Resonance Predictions from the Quark Model

S. Capstick and W. Roberts, Phys. Rev. D **47** (1993), 1994-2010.

Model state	$\lvert A_{N\pi}\rvert$ ($\mathrm{MeV}^{\frac{1}{2}}$)	$N\pi$ state assignment	Rating	$\sqrt{\Gamma_{\rm tot}}(\mathrm{BR})_{N\pi}$ ($\mathrm{MeV}^{\frac{1}{2}}$)
$[N\frac{1}{2}^+]_2(1540)$	$20.3^{+0.8}_{-0.9}$	$N\frac{1}{2}^+(1440)$	****	19.9 ± 3.0
$[N\frac{1}{2}^+]_3(1770)$	4.2 ± 0.1	$N\frac{1}{2}^+(1710)$	***	4.7 ± 1.2
$[N\frac{1}{2}^+]_4(1880)$	$2.7^{+0.6}_{-0.9}$			
$[N\frac{1}{2}^+]_5(1975)$	$2.0^{+0.2}_{-0.3}$			
$[\Delta\frac{3}{2}^+]_1(1230)$	10.4 ± 0.1	$\Delta\frac{3}{2}^+(1232)$	****	10.7 ± 0.3
$[\Delta\frac{3}{2}^+]_2(1795)$	8.7 ± 0.2	$\Delta\frac{3}{2}^+(1600)$	**	7.6 ± 2.3
$[\Delta\frac{3}{2}^+]_3(1915)$	4.2 ± 0.3	$\Delta\frac{3}{2}^+(1920)$	***	7.7 ± 2.3
$[\Delta\frac{3}{2}^+]_4(1985)$	$3.3^{+0.8}_{-1.1}$			

Nucleon and Delta Resonance Predictions from the Quark Model

S. Capstick and W. Roberts, Phys. Rev. D **47** (1993), 1994-2010.

Model state	$\lvert A_{N\pi}\rvert$ $(\mathrm{MeV}^{\frac{1}{2}})$	$N\pi$ state assignment	Rating	$\sqrt{\Gamma_{\mathrm{tot}}}(\mathrm{BR})_{N\pi}$ $(\mathrm{MeV}^{\frac{1}{2}})$
$[N\frac{1}{2}^+]_2(\cancel{1540})$ 1900	$20.3^{+0.8}_{-0.9}$	$N\frac{1}{2}^+(1440)$	****	19.9 ± 3.0
$[N\frac{1}{2}^+]_3(1770)$	4.2 ± 0.1	$N\frac{1}{2}^+(1710)$	***	4.7 ± 1.2
$[N\frac{1}{2}^+]_4(1880)$	$2.7^{+0.6}_{-0.9}$			
$[N\frac{1}{2}^+]_5(1975)$	$2.0^{+0.2}_{-0.3}$			
$[\Delta\frac{3}{2}^+]_1(1230)$	10.4 ± 0.1	$\Delta\frac{3}{2}^+(1232)$	****	10.7 ± 0.3
$[\Delta\frac{3}{2}^+]_2(1795)$	8.7 ± 0.2	$\Delta\frac{3}{2}^+(1600)$	**	7.6 ± 2.3
$[\Delta\frac{3}{2}^+]_3(1915)$	4.2 ± 0.3	$\Delta\frac{3}{2}^+(1920)$	***	7.7 ± 2.3
$[\Delta\frac{3}{2}^+]_4(1985)$	$3.3^{+0.8}_{-1.1}$			

Nucleon and Delta Resonance Predictions from the Quark Model

S. Capstick and W. Roberts, Phys. Rev. D **47** (1993), 1994-2010.

Model state	$\lvert A_{N\pi} \rvert$ (MeV$^{\frac{1}{2}}$)	$N\pi$ state assignment	Rating	$\sqrt{\Gamma_{tot}}(BR)_{N\pi}$ (MeV$^{\frac{1}{2}}$)
$[N\frac{1}{2}^+]_2(\cancel{1540})$ 1900	$20.3^{+0.8}_{-0.9}$	$N\frac{1}{2}^+(1440)$	****	19.9±3.0
$[N\frac{1}{2}^+]_3(\cancel{1770})$ 2600	4.2 ± 0.1	$N\frac{1}{2}^+(1710)$	***	4.7±1.2
$[N\frac{1}{2}^+]_4(1880)$	$2.7^{+0.6}_{-0.9}$			
$[N\frac{1}{2}^+]_5(1975)$	$2.0^{+0.2}_{-0.3}$			
$[\Delta\frac{3}{2}^+]_1(1230)$	10.4 ± 0.1	$\Delta\frac{3}{2}^+(1232)$	****	10.7±0.3
$[\Delta\frac{3}{2}^+]_2(1795)$	8.7 ± 0.2	$\Delta\frac{3}{2}^+(1600)$	**	7.6±2.3
$[\Delta\frac{3}{2}^+]_3(1915)$	4.2 ± 0.3	$\Delta\frac{3}{2}^+(1920)$	***	7.7±2.3
$[\Delta\frac{3}{2}^+]_4(1985)$	$3.3^{+0.8}_{-1.1}$			

Nucleon and Delta Resonance Predictions from the Quark Model

S. Capstick and W. Roberts, Phys. Rev. D **47** (1993), 1994-2010.

Model state	$\lvert A_{N\pi}\rvert$ (MeV$^{\frac{1}{2}}$)	$N\pi$ state assignment	Rating	$\sqrt{\Gamma_{tot}}(\mathrm{BR})_{N\pi}$ (MeV$^{\frac{1}{2}}$)
$[N\frac{1}{2}^+]_2(\cancel{1540})$ 1900	$20.3^{+0.8}_{-0.9}$	$N\frac{1}{2}^+(1440)$	****	19.9±3.0
$[N\frac{1}{2}^+]_3(\cancel{1770})$ 2600	4.2 ± 0.1	$N\frac{1}{2}^+(1710)$	***	4.7±1.2
$[N\frac{1}{2}^+]_4(\cancel{1880})$ 3600	$2.7^{+0.6}_{-0.9}$			
$[N\frac{1}{2}^+]_5(1975)$	$2.0^{+0.2}_{-0.3}$			
$[\Delta\frac{3}{2}^+]_1(1230)$	10.4 ± 0.1	$\Delta\frac{3}{2}^+(1232)$	****	10.7±0.3
$[\Delta\frac{3}{2}^+]_2(1795)$	8.7 ± 0.2	$\Delta\frac{3}{2}^+(1600)$	**	7.6±2.3
$[\Delta\frac{3}{2}^+]_3(1915)$	4.2 ± 0.3	$\Delta\frac{3}{2}^+(1920)$	***	7.7±2.3
$[\Delta\frac{3}{2}^+]_4(1985)$	$3.3^{+0.8}_{-1.1}$			

Nucleon and Delta Resonance Predictions from the Quark Model

S. Capstick and W. Roberts, Phys. Rev. D **47** (1993), 1994-2010.

Model state	$\lvert A_{N\pi}\rvert$ (MeV$^{\frac{1}{2}}$)	$N\pi$ state assignment	Rating	$\sqrt{\Gamma_{\rm tot}}(\mathrm{BR})_{N\pi}$ (MeV$^{\frac{1}{2}}$)
$[N\frac{1}{2}^+]_2(\cancel{1540})$ 1900	$20.3^{+0.8}_{-0.9}$	$N\frac{1}{2}^+(1440)$	****	19.9 ± 3.0
$[N\frac{1}{2}^+]_3(\cancel{1770})$ 2600	4.2 ± 0.1	$N\frac{1}{2}^+(1710)$	***	4.7 ± 1.2
$[N\frac{1}{2}^+]_4(\cancel{1880})$ 3600	$2.7^{+0.6}_{-0.9}$			
$[N\frac{1}{2}^+]_5(1975)$	$2.0^{+0.2}_{-0.3}$			
$[\Delta\frac{3}{2}^+]_1(1230)$	10.4 ± 0.1	$\Delta\frac{3}{2}^+(1232)$	****	10.7 ± 0.3
$[\Delta\frac{3}{2}^+]_2(1795)$	8.7 ± 0.2	$\Delta\frac{3}{2}^+(1600)$	**	7.6 ± 2.3
$[\Delta\frac{3}{2}^+]_3(1915)$	4.2 ± 0.3	$\Delta\frac{3}{2}^+(1920)$	***	7.7 ± 2.3
$[\Delta\frac{3}{2}^+]_4(1985)$	$3.3^{+0.8}_{-1.1}$			

Nucleon and Delta Resonance Predictions from the Quark Model

S. Capstick and W. Roberts, Phys. Rev. D **47** (1993), 1994-2010.

Model state	$\lvert A_{N\pi}\rvert$ (MeV$^{\frac{1}{2}}$)	$N\pi$ state assignment	Rating	$\sqrt{\Gamma_{\text{tot}}}(\text{BR})_{N\pi}$ (MeV$^{\frac{1}{2}}$)
$[N\frac{1}{2}^+]_2(\cancel{1540})$ 1900	$20.3^{+0.8}_{-0.9}$	$N\frac{1}{2}^+(1440)$	****	19.9±3.0
$[N\frac{1}{2}^+]_3(\cancel{1770})$ 2600	4.2 ± 0.1	$N\frac{1}{2}^+(1710)$	***	4.7±1.2
$[N\frac{1}{2}^+]_4(\cancel{1880})$ 3600	$2.7^{+0.6}_{-0.9}$			
$[N\frac{1}{2}^+]_5(1975)$	$2.0^{+0.2}_{-0.3}$			
$[\Delta\frac{3}{2}^+]_1(1230)$	10.4 ± 0.1	$\Delta\frac{3}{2}^+(1232)$	****	10.7±0.3
$[\Delta\frac{3}{2}^+]_2(\cancel{1795})$ 2140	8.7 ± 0.2	$\Delta\frac{3}{2}^+(1600)$	**	7.6±2.3
$[\Delta\frac{3}{2}^+]_3(1915)$	4.2 ± 0.3	$\Delta\frac{3}{2}^+(1920)$	***	7.7±2.3
$[\Delta\frac{3}{2}^+]_4(1985)$	$3.3^{+0.8}_{-1.1}$			

Nucleon and Delta Resonance Predictions from the Quark Model

S. Capstick and W. Roberts, Phys. Rev. D **47** (1993), 1994-2010.

Model state	$\lvert A_{N\pi}\rvert$ (MeV$^{\frac{1}{2}}$)	$N\pi$ state assignment	Rating	$\sqrt{\Gamma_{\rm tot}}(\mathrm{BR})_{N\pi}$ (MeV$^{\frac{1}{2}}$)
$[N\frac{1}{2}^+]_2(\cancel{1540})$ 1900	$20.3^{+0.8}_{-0.9}$	$N\frac{1}{2}^+(1440)$	****	19.9 ± 3.0
$[N\frac{1}{2}^+]_3(\cancel{1770})$ 2600	4.2 ± 0.1	$N\frac{1}{2}^+(1710)$	***	4.7 ± 1.2
$[N\frac{1}{2}^+]_4(\cancel{1880})$ 3600	$2.7^{+0.6}_{-0.9}$			
$[N\frac{1}{2}^+]_5(1975)$	$2.0^{+0.2}_{-0.3}$			
$[\Delta\frac{3}{2}^+]_1(1230)$ ✓	10.4 ± 0.1	$\Delta\frac{3}{2}^+(1232)$	****	10.7 ± 0.3
$[\Delta\frac{3}{2}^+]_2(\cancel{1795})$ 2140	8.7 ± 0.2	$\Delta\frac{3}{2}^+(1600)$	**	7.6 ± 2.3
$[\Delta\frac{3}{2}^+]_3(\cancel{1915})$ 3100	4.2 ± 0.3	$\Delta\frac{3}{2}^+(1920)$	***	7.7 ± 2.3
$[\Delta\frac{3}{2}^+]_4(1985)$	$3.3^{+0.8}_{-1.1}$			

Nucleon and Delta Resonance Predictions from the Quark Model

S. Capstick and W. Roberts, Phys. Rev. D **47** (1993), 1994-2010.

Model state	$\lvert A_{N\pi}\rvert$ (MeV$^{\frac{1}{2}}$)	$N\pi$ state assignment	Rating	$\sqrt{\Gamma_{\text{tot}}}(\text{BR})_{N\pi}$ (MeV$^{\frac{1}{2}}$)
$[N\frac{1}{2}^+]_2(\cancel{1540})$ 1900	$20.3^{+0.8}_{-0.9}$	$N\frac{1}{2}^+(1440)$	****	19.9 ± 3.0
$[N\frac{1}{2}^+]_3(\cancel{1770})$ 2600	4.2 ± 0.1	$N\frac{1}{2}^+(1710)$	***	4.7 ± 1.2
$[N\frac{1}{2}^+]_4(\cancel{1880})$ 3600	$2.7^{+0.6}_{-0.9}$			
$[N\frac{1}{2}^+]_5(1975)$	$2.0^{+0.2}_{-0.3}$			
$[\Delta\frac{3}{2}^+]_1(1230)$	10.4 ± 0.1	$\Delta\frac{3}{2}^+(1232)$	****	10.7 ± 0.3
$[\Delta\frac{3}{2}^+]_2(\cancel{1795})$ 2140	8.7 ± 0.2	$\Delta\frac{3}{2}^+(1600)$	**	7.6 ± 2.3
$[\Delta\frac{3}{2}^+]_3(\cancel{1915})$ 3100	4.2 ± 0.3	$\Delta\frac{3}{2}^+(1920)$	***	7.7 ± 2.3
$[\Delta\frac{3}{2}^+]_4(1985)$	$3.3^{+0.8}_{-1.1}$			

Nucleon and Delta Resonance Predictions from the Quark Model

S. Capstick and W. Roberts, Phys. Rev. D **47** (1993), 1994-2010.

Model state	$\lvert A_{N\pi}\rvert$ $(\mathrm{MeV}^{\frac{1}{2}})$	$N\pi$ state assignment	Rating	$\sqrt{\Gamma_{\mathrm{tot}}}(\mathrm{BR})_{N\pi}$ $(\mathrm{MeV}^{\frac{1}{2}})$
$[N\frac{1}{2}^+]_2(\cancel{1540})$ 1900	$20.3^{+0.8}_{-0.9}$	$N\frac{1}{2}^+(1440)$	****	19.9 ± 3.0
$[N\frac{1}{2}^+]_3(\cancel{1770})$ 2600	4.2 ± 0.1	$N\frac{1}{2}^+(1710)$	***	4.7 ± 1.2
$[N\frac{1}{2}^+]_4(\cancel{1880})$ 3600	$2.7^{+0.6}_{-0.9}$			
$[N\frac{1}{2}^+]_5(1975)$	$2.0^{+0.2}_{-0.3}$			
$[\Delta\frac{3}{2}^+]_1(1230)$	10.4 ± 0.1	$\Delta\frac{3}{2}^+(1232)$	****	10.7 ± 0.3
$[\Delta\frac{3}{2}^+]_2(\cancel{1795})$ 2140	8.7 ± 0.2	$\Delta\frac{3}{2}^+(1600)$	**	7.6 ± 2.3
$[\Delta\frac{3}{2}^+]_3(\cancel{1915})$ 3100	4.2 ± 0.3	$\Delta\frac{3}{2}^+(1920)$	***	7.7 ± 2.3
$[\Delta\frac{3}{2}^+]_4(1985)$	$3.3^{+0.8}_{-1.1}$			

Nucleon and Delta Resonance Predictions from the Quark Model

S. Capstick and W. Roberts, Phys. Rev. D **47** (1993), 1994-2010.

Model state	$\lvert A_{N\pi}\rvert$ (MeV$^{\frac{1}{2}}$)	$N\pi$ state assignment	Rating	$\sqrt{\Gamma_{tot}}(\mathrm{BR})_{N\pi}$ (MeV$^{\frac{1}{2}}$)
$[N\frac{1}{2}^+]_2(\cancel{1540})$ 1900	$20.3^{+0.8}_{-0.9}$	$N\frac{1}{2}^+(1440)$	****	19.9±3.0
$[N\frac{1}{2}^+]_3(\cancel{1770})$ 2600	4.2 ± 0.1	$N\frac{1}{2}^+(1710)$	***	4.7±1.2
$[N\frac{1}{2}^+]_4(\cancel{1880})$ 3600	$2.7^{+0.6}_{-0.9}$			
$[N\frac{1}{2}^+]_5(1975)$	$2.0^{+0.2}_{-0.3}$			
$[\Delta\frac{3}{2}^+]_1(1230)$ ✓	10.4 ± 0.1	$\Delta\frac{3}{2}^+(1232)$	****	10.7±0.3
$[\Delta\frac{3}{2}^+]_2(\cancel{1795})$ 2140	8.7 ± 0.2	$\Delta\frac{3}{2}^+(1600)$	**	7.6±2.3
$[\Delta\frac{3}{2}^+]_3(\cancel{1915})$ 3100	4.2 ± 0.3	$\Delta\frac{3}{2}^+(1920)$	***	7.7±2.3
$[\Delta\frac{3}{2}^+]_4(1985)$	$3.3^{+0.8}_{-1.1}$			

Section 7

Conclusions

Conclusions

- Hamiltonian Effective Field Theory (HEFT)
  - Connects scattering observables to finite-volume Lattice QCD.

Conclusions

- Hamiltonian Effective Field Theory (HEFT)
  - Connects scattering observables to finite-volume Lattice QCD.
  - Connects results at different quark masses within a single formalism.

Conclusions

- Hamiltonian Effective Field Theory (HEFT)
  - Connects scattering observables to finite-volume Lattice QCD.
  - Connects results at different quark masses within a single formalism.
  - Provides insight into the composition of energy eigenstates and lattice QCD.

Conclusions

- Hamiltonian Effective Field Theory (HEFT)
  - Connects scattering observables to finite-volume Lattice QCD.
  - Connects results at different quark masses within a single formalism.
  - Provides insight into the composition of energy eigenstates and lattice QCD.
- Simple harmonic-oscillator style spectrum structure is observed in lattice QCD.

Conclusions

- Hamiltonian Effective Field Theory (HEFT)
  - Connects scattering observables to finite-volume Lattice QCD.
  - Connects results at different quark masses within a single formalism.
  - Provides insight into the composition of energy eigenstates and lattice QCD.
- Simple harmonic-oscillator style spectrum structure is observed in lattice QCD.
- With lattice QCD constraints, HEFT provides new insight into resonance structure.
  - The $\Delta(1600)$ is dynamically generated in πN and $\pi\Delta$ rescattering.

Conclusions

- Hamiltonian Effective Field Theory (HEFT)
  - Connects scattering observables to finite-volume Lattice QCD.
  - Connects results at different quark masses within a single formalism.
  - Provides insight into the composition of energy eigenstates and lattice QCD.
- Simple harmonic-oscillator style spectrum structure is observed in lattice QCD.
- With lattice QCD constraints, HEFT provides new insight into resonance structure.
  - The $\Delta(1600)$ is dynamically generated in πN and $\pi\Delta$ rescattering.
  - The $\Delta(1920)$ is associated with the $2s$ quark-model single-particle basis state.

Conclusions

- Hamiltonian Effective Field Theory (HEFT)
  - Connects scattering observables to finite-volume Lattice QCD.
  - Connects results at different quark masses within a single formalism.
  - Provides insight into the composition of energy eigenstates and lattice QCD.
- Simple harmonic-oscillator style spectrum structure is observed in lattice QCD.
- With lattice QCD constraints, HEFT provides new insight into resonance structure.
  - The $\Delta(1600)$ is dynamically generated in πN and $\pi\Delta$ rescattering.
  - The $\Delta(1920)$ is associated with the $2s$ quark-model single-particle basis state.
  - The $N(1440)$ Roper is dynamically generated in πN, $\pi\Delta$, and σN rescattering.

Conclusions

- Hamiltonian Effective Field Theory (HEFT)
  - Connects scattering observables to finite-volume Lattice QCD.
  - Connects results at different quark masses within a single formalism.
  - Provides insight into the composition of energy eigenstates and lattice QCD.
- Simple harmonic-oscillator style spectrum structure is observed in lattice QCD.
- With lattice QCD constraints, HEFT provides new insight into resonance structure.
  - The $\Delta(1600)$ is dynamically generated in πN and $\pi\Delta$ rescattering.
  - The $\Delta(1920)$ is associated with the $2s$ quark-model single-particle basis state.
  - The $N(1440)$ Roper is dynamically generated in πN, $\pi\Delta$, and σN rescattering.
  - The $N(1710)$ and $N(1880)$ are associated with the $2s$ quark-model basis state.

Conclusions

- Hamiltonian Effective Field Theory (HEFT)
  - Connects scattering observables to finite-volume Lattice QCD.
  - Connects results at different quark masses within a single formalism.
  - Provides insight into the composition of energy eigenstates and lattice QCD.
- Simple harmonic-oscillator style spectrum structure is observed in lattice QCD.
- With lattice QCD constraints, HEFT provides new insight into resonance structure.
  - The $\Delta(1600)$ is dynamically generated in πN and $\pi\Delta$ rescattering.
  - The $\Delta(1920)$ is associated with the $2s$ quark-model single-particle basis state.
  - The $N(1440)$ Roper is dynamically generated in πN, $\pi\Delta$, and σN rescattering.
  - The $N(1710)$ and $N(1880)$ are associated with the $2s$ quark-model basis state.
- $\Lambda \frac{1}{2}^-$ resonances:
  - The $\Lambda(1405)$ has a two-pole structure generated by $\pi\Sigma$ and $\bar{K}N$ rescattering.

Conclusions

- Hamiltonian Effective Field Theory (HEFT)
  - Connects scattering observables to finite-volume Lattice QCD.
  - Connects results at different quark masses within a single formalism.
  - Provides insight into the composition of energy eigenstates and lattice QCD.
- Simple harmonic-oscillator style spectrum structure is observed in lattice QCD.
- With lattice QCD constraints, HEFT provides new insight into resonance structure.
  - The $\Delta(1600)$ is dynamically generated in πN and $\pi\Delta$ rescattering.
  - The $\Delta(1920)$ is associated with the $2s$ quark-model single-particle basis state.
  - The $N(1440)$ Roper is dynamically generated in πN, $\pi\Delta$, and σN rescattering.
  - The $N(1710)$ and $N(1880)$ are associated with the $2s$ quark-model basis state.
- $\Lambda\frac{1}{2}^-$ resonances:
  - The $\Lambda(1405)$ has a two-pole structure generated by $\pi\Sigma$ and $\bar{K}N$ rescattering.
  - The $\Lambda(1670)$ is associated with a quark-model-like single-particle basis state.

Conclusions

- Hamiltonian Effective Field Theory (HEFT)
  - Connects scattering observables to finite-volume Lattice QCD.
  - Connects results at different quark masses within a single formalism.
  - Provides insight into the composition of energy eigenstates and lattice QCD.
- Simple harmonic-oscillator style spectrum structure is observed in lattice QCD.
- With lattice QCD constraints, HEFT provides new insight into resonance structure.
  - The $\Delta(1600)$ is dynamically generated in πN and $\pi\Delta$ rescattering.
  - The $\Delta(1920)$ is associated with the $2s$ quark-model single-particle basis state.
  - The $N(1440)$ Roper is dynamically generated in πN, $\pi\Delta$, and σN rescattering.
  - The $N(1710)$ and $N(1880)$ are associated with the $2s$ quark-model basis state.
- $\Lambda\frac{1}{2}^-$ resonances:
  - The $\Lambda(1405)$ has a two-pole structure generated by $\pi\Sigma$ and $\bar{K}N$ rescattering.
  - The $\Lambda(1670)$ is associated with a quark-model-like single-particle basis state.
- These results provide a novel solution to the missing baryon resonances problem.

Section 8

Supplementary Information

Two different descriptions of the Roper resonance

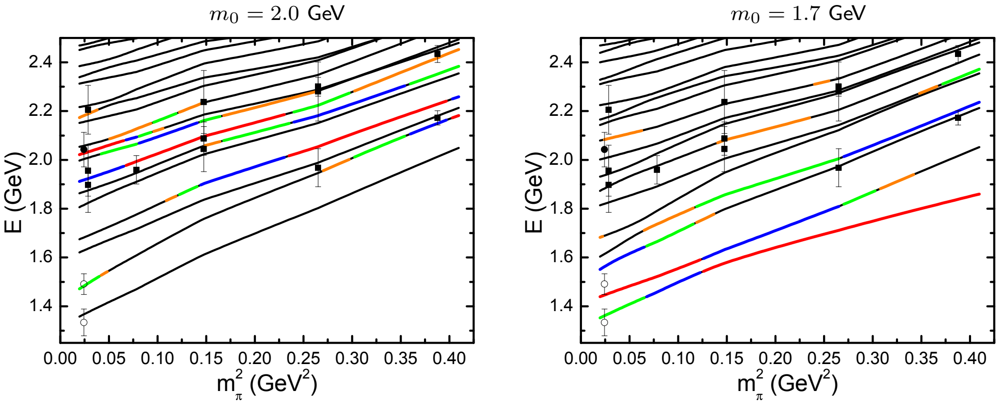

(left) Resonance generated by strong rescattering in meson-baryon channels.
(right) Meson dressings of a quark-model like core.

Score Card

Criteria	$m_0 = 1.7$ GeV	$m_0 = 2.0$ GeV
Describes experimental data well.		

Score Card

Criteria	$m_0 = 1.7$ GeV	$m_0 = 2.0$ GeV
Describes experimental data well.	✔	✔

Score Card

Criteria	$m_0 = 1.7$ GeV	$m_0 = 2.0$ GeV
Describes experimental data well.	✔	✔
Produces poles in accord with PDG.		

Score Card

Criteria	$m_0 = 1.7$ GeV	$m_0 = 2.0$ GeV
Describes experimental data well.	✔	✔
Produces poles in accord with PDG.	✔	✔

Score Card

Criteria	$m_0 = 1.7$ GeV	$m_0 = 2.0$ GeV
Describes experimental data well.	✔	✔
Produces poles in accord with PDG.	✔	✔
1st lattice scattering state created via σN interpolator has dominant $\langle\, \sigma N \mid E_1 \,\rangle$ in HEFT.		

Score Card

Criteria	$m_0 = 1.7$ GeV	$m_0 = 2.0$ GeV
Describes experimental data well.	✔	✔
Produces poles in accord with PDG.	✔	✔
1st lattice scattering state created via σN interpolator has dominant $\langle\, \sigma N \mid E_1 \,\rangle$ in HEFT.	✔	✔

Score Card

Criteria	$m_0 = 1.7$ GeV	$m_0 = 2.0$ GeV
Describes experimental data well.	✔	✔
Produces poles in accord with PDG.	✔	✔
1st lattice scattering state created via σN interpolator has dominant $\langle\, \sigma N \,\vert\, E_1 \,\rangle$ in HEFT.	✔	✔
2nd lattice scattering state created via πN interpolator has dominant $\langle\, \pi N \,\vert\, E_2 \,\rangle$ in HEFT.		

Score Card

Criteria	$m_0 = 1.7$ GeV	$m_0 = 2.0$ GeV
Describes experimental data well.	✔	✔
Produces poles in accord with PDG.	✔	✔
1^{st} lattice scattering state created via σN interpolator has dominant $\langle\, \sigma N \,\vert\, E_1 \,\rangle$ in HEFT.	✔	✔
2^{nd} lattice scattering state created via πN interpolator has dominant $\langle\, \pi N \,\vert\, E_2 \,\rangle$ in HEFT.	✗	✔

Score Card

Criteria	$m_0 = 1.7$ GeV	$m_0 = 2.0$ GeV
Describes experimental data well.	✔	✔
Produces poles in accord with PDG.	✔	✔
1st lattice scattering state created via σN interpolator has dominant $\langle\, \sigma N \,\vert\, E_1 \,\rangle$ in HEFT.	✔	✔
2nd lattice scattering state created via πN interpolator has dominant $\langle\, \pi N \,\vert\, E_2 \,\rangle$ in HEFT.	✗	✔
L-QCD states excited with 3-quark ops. are associated with HEFT states with large $\langle\, B_0 \,\vert\, E_\alpha \,\rangle$.		

Score Card

Criteria	$m_0 = 1.7$ GeV	$m_0 = 2.0$ GeV
Describes experimental data well.	✔	✔
Produces poles in accord with PDG.	✔	✔
1st lattice scattering state created via σN interpolator has dominant $\langle\, \sigma N \,|\, E_1 \,\rangle$ in HEFT.	✔	✔
2nd lattice scattering state created via πN interpolator has dominant $\langle\, \pi N \,|\, E_2 \,\rangle$ in HEFT.	✗	✔
L-QCD states excited with 3-quark ops. are associated with HEFT states with large $\langle\, B_0 \,|\, E_\alpha \,\rangle$.	✗	✔

Score Card

Criteria	$m_0 = 1.7$ GeV	$m_0 = 2.0$ GeV
Describes experimental data well.	✔	✔
Produces poles in accord with PDG.	✔	✔
1st lattice scattering state created via σN interpolator has dominant $\langle\, \sigma N \,\vert\, E_1 \,\rangle$ in HEFT.	✔	✔
2nd lattice scattering state created via πN interpolator has dominant $\langle\, \pi N \,\vert\, E_2 \,\rangle$ in HEFT.	✗	✔
L-QCD states excited with 3-quark ops. are associated with HEFT states with large $\langle\, B_0 \,\vert\, E_\alpha \,\rangle$.	✗	✔
HEFT predicts three-quark states that exist in lattice QCD.		

Score Card

Criteria	$m_0 = 1.7$ GeV	$m_0 = 2.0$ GeV
Describes experimental data well.	✔	✔
Produces poles in accord with PDG.	✔	✔
1st lattice scattering state created via σN interpolator has dominant $\langle\, \sigma N \,\vert\, E_1 \,\rangle$ in HEFT.	✔	✔
2nd lattice scattering state created via πN interpolator has dominant $\langle\, \pi N \,\vert\, E_2 \,\rangle$ in HEFT.	✗	✔
L-QCD states excited with 3-quark ops. are associated with HEFT states with large $\langle\, B_0 \,\vert\, E_\alpha \,\rangle$.	✗	✔
HEFT predicts three-quark states that exist in lattice QCD.	✗	✔

Conclusion

- The Roper resonance is not associated with a low-lying three-quark core.

Conclusion

- The Roper resonance is not associated with a low-lying three-quark core.
- The Roper resonance is generated by strong rescattering in meson-baryon channels.

Conclusion

- The Roper resonance is not associated with a low-lying three-quark core.
- The Roper resonance is generated by strong rescattering in meson-baryon channels.

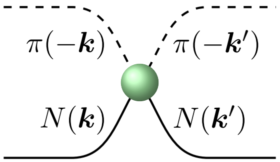

Conclusion

- The Roper resonance is not associated with a low-lying three-quark core.
- The Roper resonance is generated by strong rescattering in meson-baryon channels.

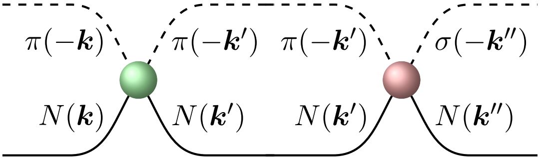

Conclusion

- The Roper resonance is not associated with a low-lying three-quark core.
- The Roper resonance is generated by strong rescattering in meson-baryon channels.

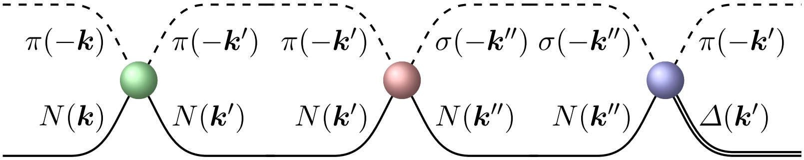

Conclusion

- The Roper resonance is not associated with a low-lying three-quark core.
- The Roper resonance is generated by strong rescattering in meson-baryon channels.

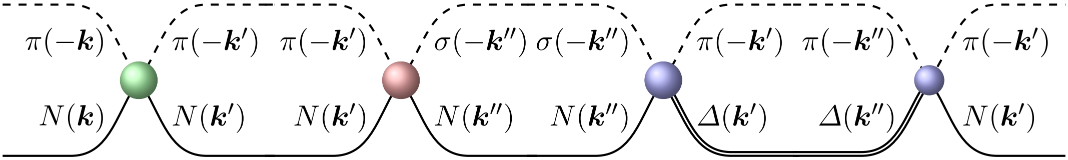

Conclusion

- The Roper resonance is not associated with a low-lying three-quark core.
- The Roper resonance is generated by strong rescattering in meson-baryon channels.

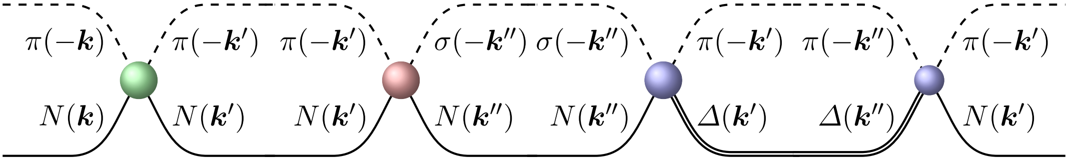

- The $2s$ excitation of the nucleon is dressed to lie at ~ 1.9 GeV

HEFT Extensions

- Formalism for partial-wave mixing in HEFT has been developed in Y. Li, J. J. Wu, C. D. Abell, D. B. L. and A. W. Thomas. Phys. Rev. D **101**, no.11, 114501 (2020) [arXiv:1910.04973 [hep-lat]]
- And extended to moving and elongated finite-volumes in Y. Li, J. J. Wu, D. B. L. and A. W. Thomas Phys. Rev. D **103** no.9, 094518 (2021) [arXiv:2103.12260 [hep-lat]].

Room for non-resonant three-body contributions in $N1/2^+$

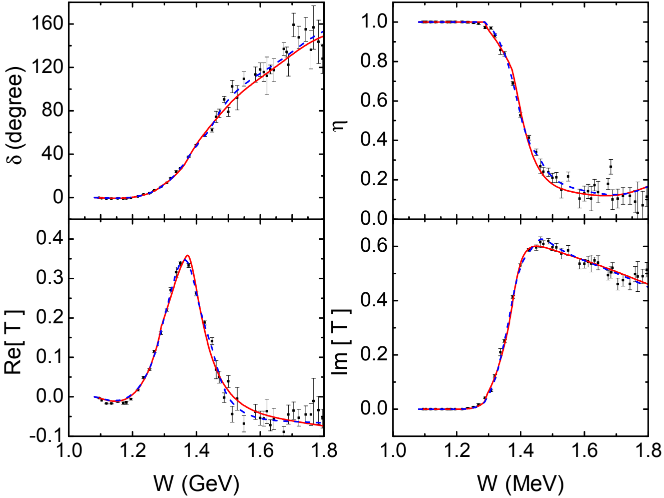

Room for non-resonant three-body contributions in $N1/2^+$

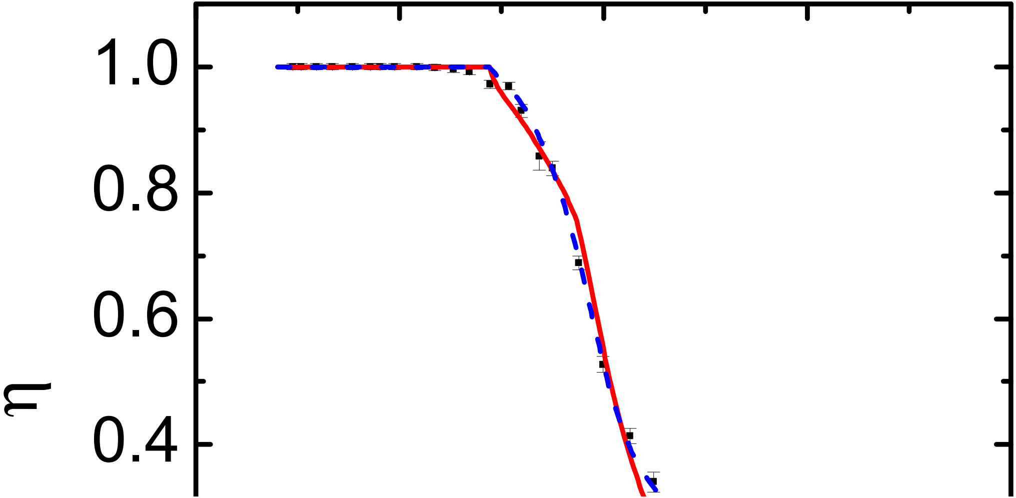

Room for non-resonant three-body contributions in $\Delta 3/2^+$

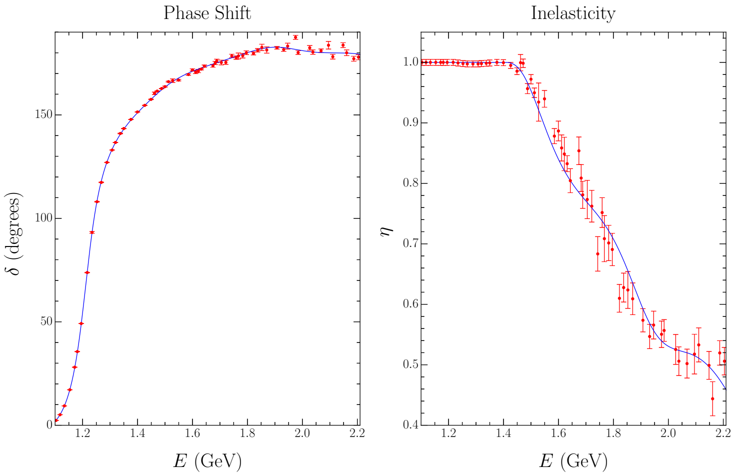

Room for non-resonant three-body contributions in $\Delta 3/2^+$

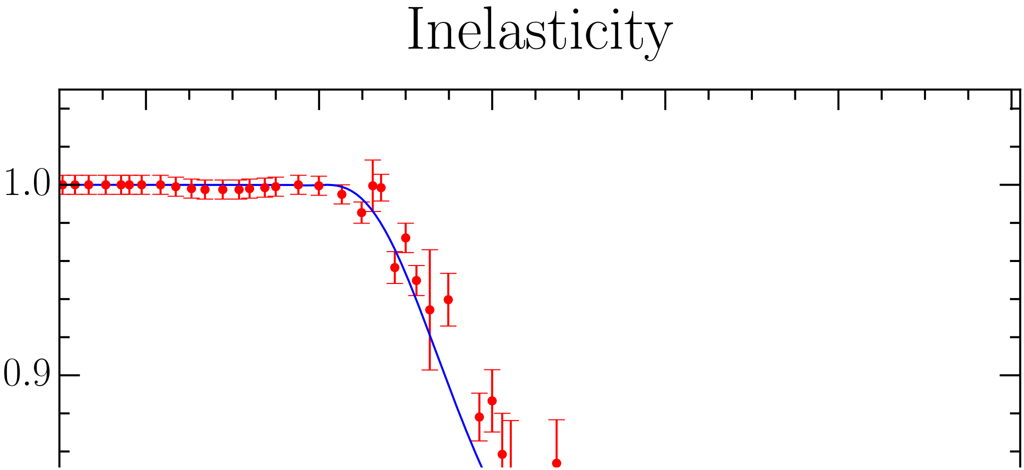

Δ Finite Volume Spectrum at $L = 3$ fm

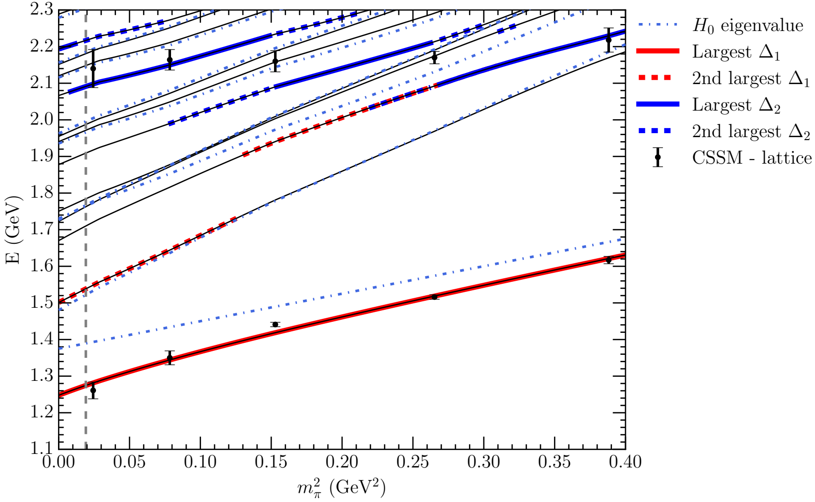

Δ Finite Volume Spectrum at $L = 3$ fm with $\pi\pi N$ states

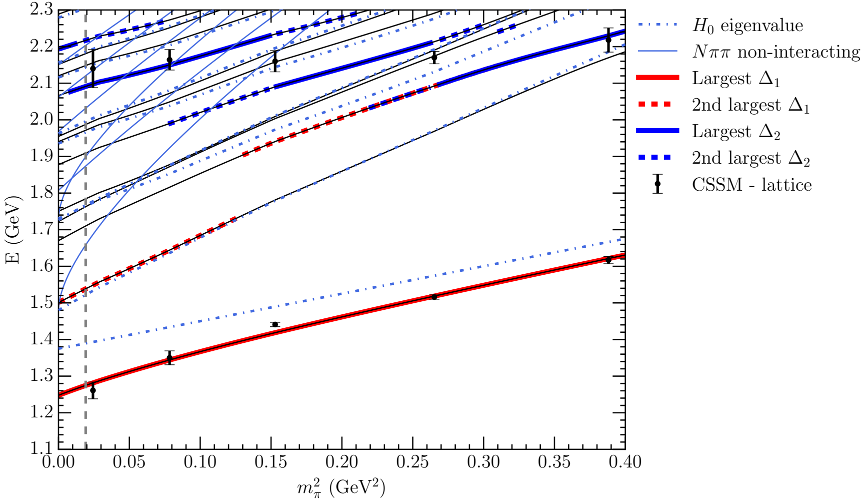

Evidence the $2s$ state is associated with the $N1/2^+(1710)$ and $N1/2^+(1880)$

- The $N1/2^+(1880)$ was observed in photoproduction while missed in πN scattering.

Evidence the $2s$ state is associated with the $N1/2^+(1710)$ and $N1/2^+(1880)$

- The $N1/2^+(1880)$ was observed in photoproduction while missed in πN scattering.
- The $N1/2^+(1710)$ has a small width of 140 MeV and perhaps as small as 80 MeV.

Evidence the $2s$ state is associated with the $N1/2^+(1710)$ and $N1/2^+(1880)$

- The $N1/2^+(1880)$ was observed in photoproduction while missed in πN scattering.
- The $N1/2^+(1710)$ has a small width of 140 MeV and perhaps as small as 80 MeV.
- Both suggest the $2s$ excitation on the lattice may be insensitive to modifications of the meson dressings.

Evidence the $2s$ state is associated with the $N1/2^+(1710)$ and $N1/2^+(1880)$

- The $N1/2^+(1880)$ was observed in photoproduction while missed in πN scattering.
- The $N1/2^+(1710)$ has a small width of 140 MeV and perhaps as small as 80 MeV.
- Both suggest the $2s$ excitation on the lattice may be insensitive to modifications of the meson dressings.
- Consider a quenched QCD simulation with matched lattice spacing and quark masses.

Evidence the $2s$ state is associated with the $N1/2^+(1710)$ and $N1/2^+(1880)$

- The $N1/2^+(1880)$ was observed in photoproduction while missed in πN scattering.
- The $N1/2^+(1710)$ has a small width of 140 MeV and perhaps as small as 80 MeV.
- Both suggest the $2s$ excitation on the lattice may be insensitive to modifications of the meson dressings.
- Consider a quenched QCD simulation with matched lattice spacing and quark masses.
  - Couplings to meson dressings are suppressed.

Evidence the $2s$ state is associated with the $N1/2^+(1710)$ and $N1/2^+(1880)$

- The $N1/2^+(1880)$ was observed in photoproduction while missed in πN scattering.
- The $N1/2^+(1710)$ has a small width of 140 MeV and perhaps as small as 80 MeV.
- Both suggest the $2s$ excitation on the lattice may be insensitive to modifications of the meson dressings.
- Consider a quenched QCD simulation with matched lattice spacing and quark masses.
    - Couplings to meson dressings are suppressed.
- Quark-model dominated states will be insensitive to quenching.

Evidence the $2s$ state is associated with the $N1/2^+(1710)$ and $N1/2^+(1880)$

- The $N1/2^+(1880)$ was observed in photoproduction while missed in πN scattering.
- The $N1/2^+(1710)$ has a small width of 140 MeV and perhaps as small as 80 MeV.
- Both suggest the $2s$ excitation on the lattice may be insensitive to modifications of the meson dressings.
- Consider a quenched QCD simulation with matched lattice spacing and quark masses.
  - Couplings to meson dressings are suppressed.
- Quark-model dominated states will be insensitive to quenching.
- Is there a state ~ 1.9 GeV that is insensitive to quenching?

Comparison of 2+1 flavour and quenched lattice simulation results

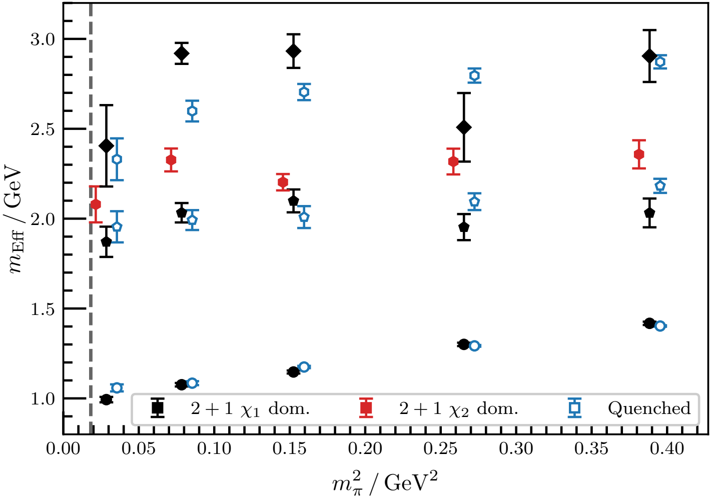

Model (in)dependence in HEFT: Lüscher formalism

- HEFT incorporates the Lüscher formalism.

Model (in)dependence in HEFT: Lüscher formalism

- HEFT incorporates the Lüscher formalism.
- It provides a rigorous relationship between the finite-volume energy spectrum and the scattering amplitudes of experiment.

Model (in)dependence in HEFT: Lüscher formalism

- HEFT incorporates the Lüscher formalism.
- It provides a rigorous relationship between the finite-volume energy spectrum and the scattering amplitudes of experiment.
- In HEFT, this relationship is mediated by a Hamiltonian.

Model (in)dependence in HEFT: Lüscher formalism

- HEFT incorporates the Lüscher formalism.
- It provides a rigorous relationship between the finite-volume energy spectrum and the scattering amplitudes of experiment.
- In HEFT, this relationship is mediated by a Hamiltonian.
- Need to have a sufficient number of tunable parameters within the Hamiltonian.

Model (in)dependence in HEFT: Lüscher formalism

- HEFT incorporates the Lüscher formalism.
- It provides a rigorous relationship between the finite-volume energy spectrum and the scattering amplitudes of experiment.
- In HEFT, this relationship is mediated by a Hamiltonian.
- Need to have a sufficient number of tunable parameters within the Hamiltonian.
- The Hamiltonian is only mediary.

Model (in)dependence in HEFT: Lüscher formalism

- HEFT incorporates the Lüscher formalism.
- It provides a rigorous relationship between the finite-volume energy spectrum and the scattering amplitudes of experiment.
- In HEFT, this relationship is mediated by a Hamiltonian.
- Need to have a sufficient number of tunable parameters within the Hamiltonian.
- The Hamiltonian is only mediary.
- However, the Lüscher formalism provides no avenue for changing the quark mass.

Model (in)dependence in HEFT - Quark mass variation

- Finite-volume HEFT reproduces finite-volume χPT in the perturbative limit by construction.

Model (in)dependence in HEFT - Quark mass variation

- Finite-volume HEFT reproduces finite-volume χPT in the perturbative limit by construction.
- In the multi scattering-channel case, the Hamiltonian becomes tightly constrained.
    - Experimental data is described accurately for only a limited range of parameters with specific regulator shapes.

Model (in)dependence in HEFT - Quark mass variation

- Finite-volume HEFT reproduces finite-volume χPT in the perturbative limit by construction.
- In the multi scattering-channel case, the Hamiltonian becomes tightly constrained.
  - Experimental data is described accurately for only a limited range of parameters with specific regulator shapes.
- The consideration of quark masses away from the physical point further constrains the Hamiltonian.

Model (in)dependence in HEFT - Quark mass variation

- Finite-volume HEFT reproduces finite-volume χPT in the perturbative limit by construction.
- In the multi scattering-channel case, the Hamiltonian becomes tightly constrained.
  - Experimental data is described accurately for only a limited range of parameters with specific regulator shapes.
- The consideration of quark masses away from the physical point further constrains the Hamiltonian.
- The Hamiltonian has become a tightly constrained model.

Model (in)dependence in HEFT - Quark mass variation

- Draw on model-independent constraints to determine the Hamiltonian.
  - Lattice QCD and experiment.

Model (in)dependence in HEFT - Quark mass variation

- Draw on model-independent constraints to determine the Hamiltonian.
  - Lattice QCD and experiment.
- One set of lattice QCD results is required to determine the quark mass dependence of the bare basis state(s).
  - A term linear in the quark mass is usually sufficient to describe lattice QCD results.

Model (in)dependence in HEFT - Quark mass variation

- Draw on model-independent constraints to determine the Hamiltonian.
  - Lattice QCD and experiment.
- One set of lattice QCD results is required to determine the quark mass dependence of the bare basis state(s).
  - A term linear in the quark mass is usually sufficient to describe lattice QCD results.
- Make predictions of the finite-volume spectrum considered by other lattice groups.
  - Different volumes and different quark masses can be addressed.

Model (in)dependence in HEFT - Quark mass variation

- Draw on model-independent constraints to determine the Hamiltonian.
  - Lattice QCD and experiment.
- One set of lattice QCD results is required to determine the quark mass dependence of the bare basis state(s).
  - A term linear in the quark mass is usually sufficient to describe lattice QCD results.
- Make predictions of the finite-volume spectrum considered by other lattice groups.
  - Different volumes and different quark masses can be addressed.
- Model independence is governed by the distance from the physical point.
  - For example, $m_\pi = 204$ MeV considered by the BaSc collaboration.

Model dependence in HEFT

- The eigenvectors describe how the non-interacting basis states come together to compose the eigenstates of the spectrum.

Model dependence in HEFT

- The eigenvectors describe how the non-interacting basis states come together to compose the eigenstates of the spectrum.
- They are model dependent.

Model dependence in HEFT

- The eigenvectors describe how the non-interacting basis states come together to compose the eigenstates of the spectrum.
- They are model dependent.
- There is little freedom in the model parameters of the Hamiltonian such that the predictions of the Hamiltonian are well defined.

Model dependence in HEFT

- The eigenvectors describe how the non-interacting basis states come together to compose the eigenstates of the spectrum.
- They are model dependent.
- There is little freedom in the model parameters of the Hamiltonian such that the predictions of the Hamiltonian are well defined.
- They are similar to the eigenvectors of lattice-QCD correlation matrices.
  - They describe the linear combination of interpolating fields isolating energy eigenstates on the lattice.

Model dependence in HEFT

- The eigenvectors describe how the non-interacting basis states come together to compose the eigenstates of the spectrum.
- They are model dependent.
- There is little freedom in the model parameters of the Hamiltonian such that the predictions of the Hamiltonian are well defined.
- They are similar to the eigenvectors of lattice-QCD correlation matrices.
  - They describe the linear combination of interpolating fields isolating energy eigenstates on the lattice.
- These too are model dependent.

Model dependence in HEFT

- The eigenvectors describe how the non-interacting basis states come together to compose the eigenstates of the spectrum.
- They are model dependent.
- There is little freedom in the model parameters of the Hamiltonian such that the predictions of the Hamiltonian are well defined.
- They are similar to the eigenvectors of lattice-QCD correlation matrices.
  - They describe the linear combination of interpolating fields isolating energy eigenstates on the lattice.
- These too are model dependent.
- However, the composition of the states drawn from the lattice correlation matrix is similar to the description provided by HEFT.

Model (in)dependence in HEFT - Summary

- There is a direct model-independent link between the scattering observables of experiment and the finite-volume spectrum calculated in HEFT.

Model (in)dependence in HEFT - Summary

- There is a direct model-independent link between the scattering observables of experiment and the finite-volume spectrum calculated in HEFT.
- Variation of the quark masses away from the physical quark mass is constrained by lattice QCD results.

Model (in)dependence in HEFT - Summary

- There is a direct model-independent link between the scattering observables of experiment and the finite-volume spectrum calculated in HEFT.
- Variation of the quark masses away from the physical quark mass is constrained by lattice QCD results.
- The Hamiltonian eigenvectors describing the basis-state composition of finite-volume energy eigenstates are model dependent.

Model (in)dependence in HEFT - Summary

- There is a direct model-independent link between the scattering observables of experiment and the finite-volume spectrum calculated in HEFT.
- Variation of the quark masses away from the physical quark mass is constrained by lattice QCD results.
- The Hamiltonian eigenvectors describing the basis-state composition of finite-volume energy eigenstates are model dependent.
- They are analogous to the interpolator dependent eigenvectors of lattice QCD correlation matrices describing the linear combination of interpolating fields isolating energy eigenstates.

Model (in)dependence in HEFT - Summary

- There is a direct model-independent link between the scattering observables of experiment and the finite-volume spectrum calculated in HEFT.
- Variation of the quark masses away from the physical quark mass is constrained by lattice QCD results.
- The Hamiltonian eigenvectors describing the basis-state composition of finite-volume energy eigenstates are model dependent.
- They are analogous to the interpolator dependent eigenvectors of lattice QCD correlation matrices describing the linear combination of interpolating fields isolating energy eigenstates.
- The similarity displayed by these two different sets of eigenvectors suggests that they do indeed provide insight into hadron structure.

The $\Lambda(1405)$ in Lattice QCD

- First observed in

  B. J. Menadue, W. Kamleh, DBL and M. S. Mahbub, Phys. Rev. Lett. **108** (2012) 112001 [arXiv:1109.6716 [hep-lat]].

The $\Lambda(1405)$ in Lattice QCD

- First observed in

  B. J. Menadue, W. Kamleh, DBL and M. S. Mahbub, Phys. Rev. Lett. **108** (2012) 112001 [arXiv:1109.6716 [hep-lat]].

- Excited by local three-quark operators.
  - A mix of two flavour-octet interpolators and a flavour-singlet operator.
  - A variety of quark distributions via smeared sources.

The $\Lambda(1405)$ in Lattice QCD

- First observed in

  B. J. Menadue, W. Kamleh, DBL and M. S. Mahbub, Phys. Rev. Lett. **108** (2012) 112001 [arXiv:1109.6716 [hep-lat]].

- Excited by local three-quark operators.
  - A mix of two flavour-octet interpolators and a flavour-singlet operator.
  - A variety of quark distributions via smeared sources.

- Appeared to be a local three quark state.
  - But a study of the strange magnetic form factor revealed an exotic structure.

Strange Magnetic Form Factor of the $\Lambda(1405)$

J. M. M. Hall, *et al.* [CSSM], Phys. Rev. Lett. **114**, 132002 (2015) arXiv:1411.3402 [hep-lat]

- Provides direct insight into the possible dominance of a molecular $\overline{K}N$ bound state.

Strange Magnetic Form Factor of the $\Lambda(1405)$

J. M. M. Hall, *et al.* [CSSM], Phys. Rev. Lett. **114**, 132002 (2015) arXiv:1411.3402 [hep-lat]

- Provides direct insight into the possible dominance of a molecular $\overline{K}N$ bound state.
- In forming such a molecular state, the $\Lambda(u,d,s)$ valence quark configuration is complemented by
  - A $u, \overline{u}$ pair making a $K^-(s,\overline{u})$ - $p(u,u,d)$ bound state, or
  - A $d, \overline{d}$ pair making a $\overline{K}^0(s,\overline{d})$ - $n(d,d,u)$ bound state.

Strange Magnetic Form Factor of the $\Lambda(1405)$

J. M. M. Hall, *et al.* [CSSM], Phys. Rev. Lett. **114**, 132002 (2015) arXiv:1411.3402 [hep-lat]

- Provides direct insight into the possible dominance of a molecular $\overline{K}N$ bound state.
- In forming such a molecular state, the $\Lambda(u, d, s)$ valence quark configuration is complemented by
  - A $u, \overline{u}$ pair making a $K^-(s, \overline{u})$ - $p(u, u, d)$ bound state, or
  - A $d, \overline{d}$ pair making a $\overline{K}^0(s, \overline{d})$ - $n(d, d, u)$ bound state.
- In both cases the strange quark is confined within a spin-0 kaon and has no preferred spin orientation.

Strange Magnetic Form Factor of the $\Lambda(1405)$

J. M. M. Hall, *et al.* [CSSM], Phys. Rev. Lett. **114**, 132002 (2015) arXiv:1411.3402 [hep-lat]

- Provides direct insight into the possible dominance of a molecular $\overline{K}N$ bound state.
- In forming such a molecular state, the $\Lambda(u,d,s)$ valence quark configuration is complemented by
  - A $u, \overline{u}$ pair making a $K^-(s,\overline{u})$ - $p(u,u,d)$ bound state, or
  - A $d, \overline{d}$ pair making a $\overline{K}^0(s,\overline{d})$ - $n(d,d,u)$ bound state.
- In both cases the strange quark is confined within a spin-0 kaon and has no preferred spin orientation.
- To conserve parity, the kaon has zero orbital angular momentum.

Strange Magnetic Form Factor of the $\Lambda(1405)$

J. M. M. Hall, *et al.* [CSSM], Phys. Rev. Lett. **114**, 132002 (2015) arXiv:1411.3402 [hep-lat]

- Provides direct insight into the possible dominance of a molecular $\overline{K}N$ bound state.
- In forming such a molecular state, the $\Lambda(u, d, s)$ valence quark configuration is complemented by
  - A $u, \overline{u}$ pair making a $K^-(s, \overline{u})$ - $p(u, u, d)$ bound state, or
  - A $d, \overline{d}$ pair making a $\overline{K}^0(s, \overline{d})$ - $n(d, d, u)$ bound state.
- In both cases the strange quark is confined within a spin-0 kaon and has no preferred spin orientation.
- To conserve parity, the kaon has zero orbital angular momentum.
- Thus, the strange quark does not contribute to the magnetic form factor of the $\Lambda(1405)$ when it is dominated by a $\overline{K}N$ molecule.

Strange Magnetic Form Factor of the $\Lambda(1405)$

J. M. M. Hall, *et al.* [CSSM], Phys. Rev. Lett. **114**, 132002 (2015) arXiv:1411.3402 [hep-lat]

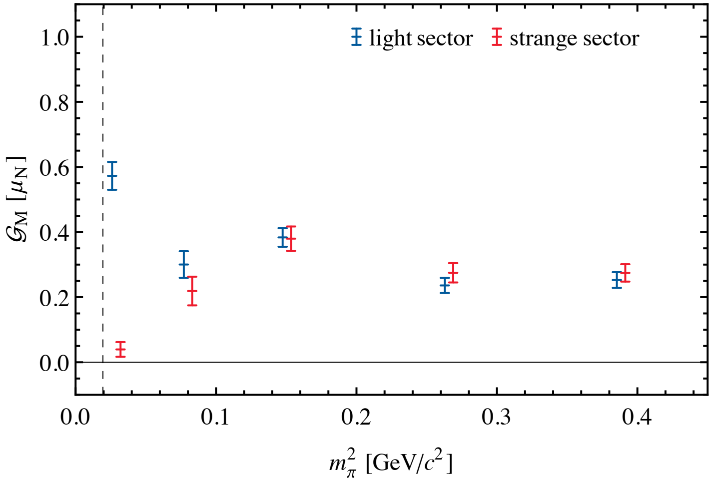

Electric form factors of the $\Lambda(1405)$ at $Q^2 \sim 0.16\,\text{GeV}^2$

B. J. Menadue, W. Kamleh, DBL, M. Selim Mahbub and B. J. Owen, PoS **LATTICE2013** (2014), 280 [arXiv:1311.5026 [hep-lat]]

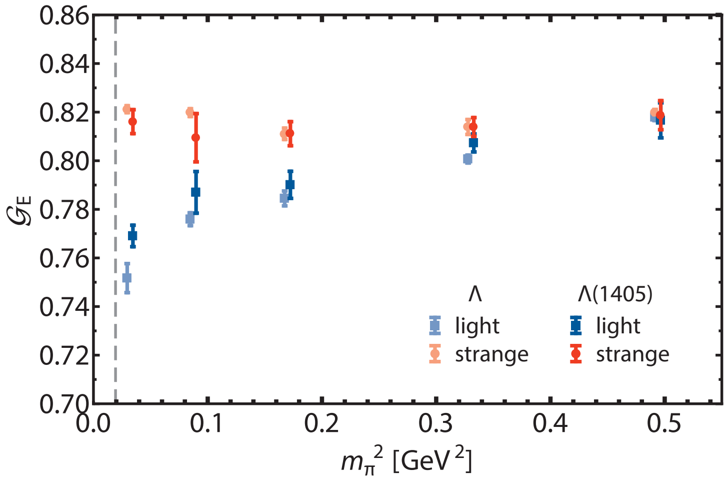

Smeared Source Correlation Functions

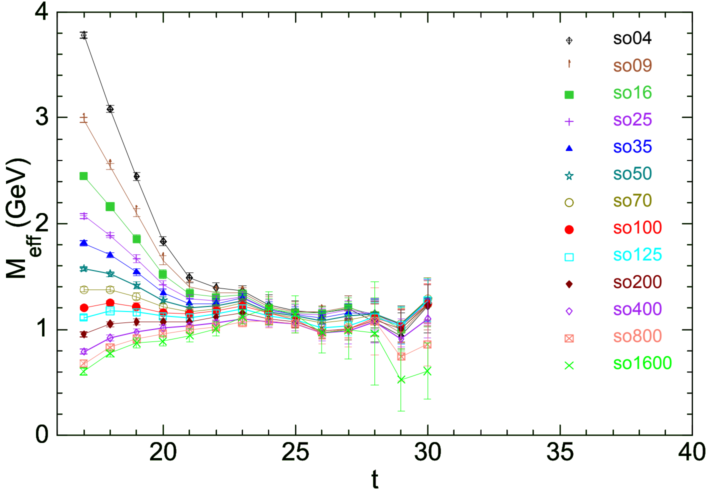

Positive Parity Nucleon Spectrum CSSM

M. S. Mahbub *et al.* [CSSM Lattice Collaboration], Phys. Lett. B **707** (2012) 389 arXiv:1011.5724 [hep-lat].

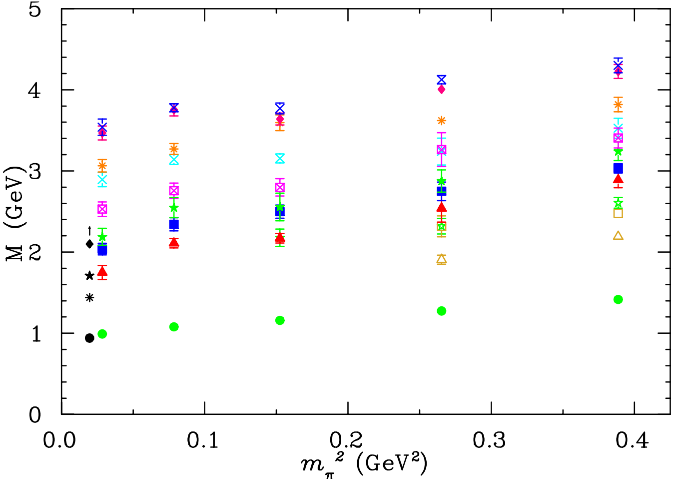

Positive Parity Nucleon Spectrum CSSM & JLab HSC

R. G. Edwards, J. J. Dudek, D. G. Richards and S. J. Wallace, Phys. Rev. D **84** (2011) 074508 arXiv:1104.5152 [hep-ph].

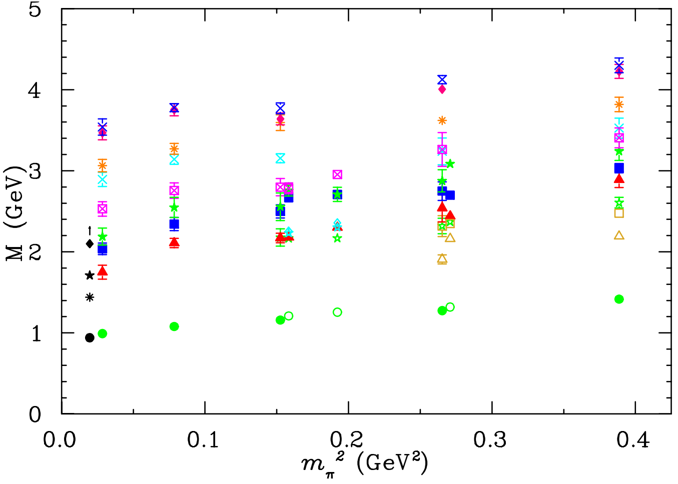

Negative Parity Nucleon Spectrum CSSM

M. S. Mahbub *et al.* [CSSM Lattice Collaboration], Phys. Lett. B **707** (2012) 389 arXiv:1011.5724 [hep-lat].

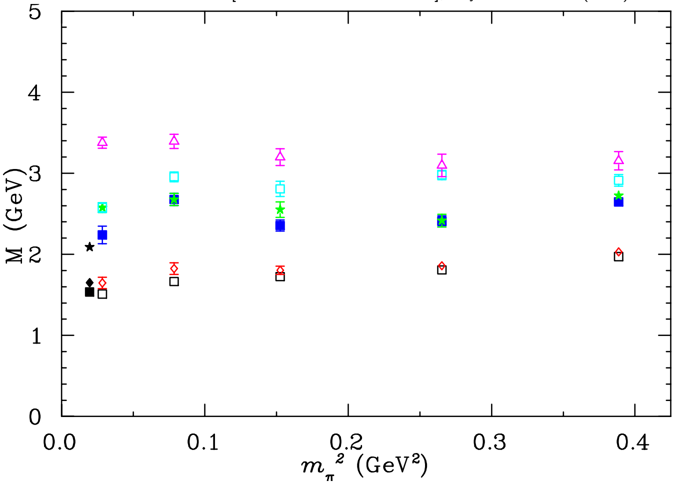

Negative Parity Nucleon Spectrum CSSM & JLab HSC

R. G. Edwards, J. J. Dudek, D. G. Richards and S. J. Wallace, Phys. Rev. D **84** (2011) 074508 arXiv:1104.5152 [hep-ph].

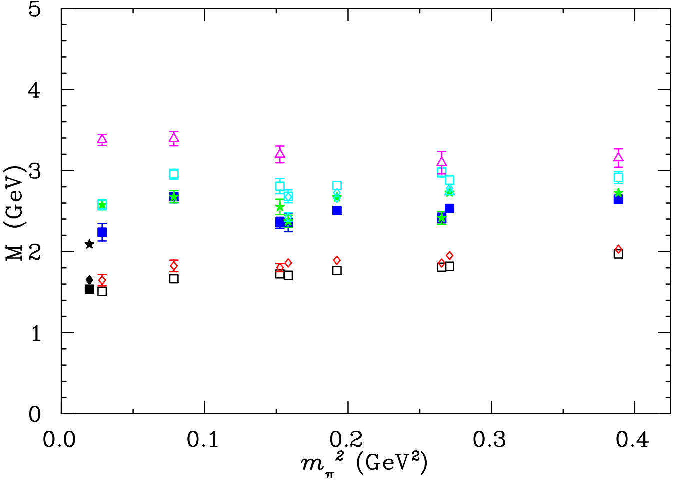

Other Calculations of the Nucleon Spectrum

- Berlin-Graz-Regensburg (BGR) collaboration

  G. P. Engel *et al.* [BGR], Phys. Rev. D **87** (2013) no.7, 074504 [arXiv:1301.4318 [hep-lat]].

  In agreement but with large uncertainties.

Other Calculations of the Nucleon Spectrum

- Berlin-Graz-Regensburg (BGR) collaboration

  G. P. Engel *et al.* [BGR], Phys. Rev. D **87** (2013) no.7, 074504 [arXiv:1301.4318 [hep-lat]].

  In agreement but with large uncertainties.

- χQCD Collaboration results

  K. F. Liu, *et al.*, "The Roper Puzzle," PoS **LATTICE2013** (2014), 507 [arXiv:1403.6847 [hep-ph]].

  Analysed the HSC correlators with their Sequential Empirical Bayesian analysis.

Other Calculations of the Nucleon Spectrum

- Berlin-Graz-Regensburg (BGR) collaboration

  G. P. Engel *et al.* [BGR], Phys. Rev. D **87** (2013) no.7, 074504 [arXiv:1301.4318 [hep-lat]].

  In agreement but with large uncertainties.

- χQCD Collaboration results

  K. F. Liu, *et al.*, "The Roper Puzzle," PoS **LATTICE2013** (2014), 507 [arXiv:1403.6847 [hep-ph]].

  Analysed the HSC correlators with their Sequential Empirical Bayesian analysis.
  - One correlator versus $28 \times 28 = 784$ correlators analysed by the HSC.

Other Calculations of the Nucleon Spectrum

- Berlin-Graz-Regensburg (BGR) collaboration

  G. P. Engel *et al.* [BGR], Phys. Rev. D **87** (2013) no.7, 074504 [arXiv:1301.4318 [hep-lat]].

  In agreement but with large uncertainties.

- χQCD Collaboration results

  K. F. Liu, *et al.*, "The Roper Puzzle," PoS **LATTICE2013** (2014), 507 [arXiv:1403.6847 [hep-ph]].

  Analysed the HSC correlators with their Sequential Empirical Bayesian analysis.
  - One correlator versus $28 \times 28 = 784$ correlators analysed by the HSC.
  - Obtained a result 300 MeV below that of the HSC.

Other Calculations of the Nucleon Spectrum

- Berlin-Graz-Regensburg (BGR) collaboration

  G. P. Engel *et al.* [BGR], Phys. Rev. D **87** (2013) no.7, 074504 [arXiv:1301.4318 [hep-lat]].

  In agreement but with large uncertainties.

- χQCD Collaboration results

  K. F. Liu, *et al.*, "The Roper Puzzle," PoS **LATTICE2013** (2014), 507 [arXiv:1403.6847 [hep-ph]].

  Analysed the HSC correlators with their Sequential Empirical Bayesian analysis.
  - One correlator versus $28 \times 28 = 784$ correlators analysed by the HSC.
  - Obtained a result 300 MeV below that of the HSC.
  - Conjectured the HSC results are wrong.
    - Their source smearing is too small to see the wave function node.

Other Calculations of the Nucleon Spectrum

- Berlin-Graz-Regensburg (BGR) collaboration

  G. P. Engel *et al.* [BGR], Phys. Rev. D **87** (2013) no.7, 074504 [arXiv:1301.4318 [hep-lat]].

  In agreement but with large uncertainties.

- χQCD Collaboration results

  K. F. Liu, *et al.*, "The Roper Puzzle," PoS **LATTICE2013** (2014), 507 [arXiv:1403.6847 [hep-ph]].

  Analysed the HSC correlators with their Sequential Empirical Bayesian analysis.
  - One correlator versus $28 \times 28 = 784$ correlators analysed by the HSC.
  - Obtained a result 300 MeV below that of the HSC.
  - Conjectured the HSC results are wrong.
    - Their source smearing is too small to see the wave function node.
  - Argument already excluded by the CSSM results.

Other Calculations of the Nucleon Spectrum

- Berlin-Graz-Regensburg (BGR) collaboration

  G. P. Engel *et al.* [BGR], Phys. Rev. D **87** (2013) no.7, 074504 [arXiv:1301.4318 [hep-lat]].

  In agreement but with large uncertainties.

- χQCD Collaboration results

  K. F. Liu, *et al.*, "The Roper Puzzle," PoS **LATTICE2013** (2014), 507 [arXiv:1403.6847 [hep-ph]].

  Analysed the HSC correlators with their Sequential Empirical Bayesian analysis.
  - One correlator versus $28 \times 28 = 784$ correlators analysed by the HSC.
  - Obtained a result 300 MeV below that of the HSC.
  - Conjectured the HSC results are wrong.
    - Their source smearing is too small to see the wave function node.
  - Argument already excluded by the CSSM results.

- Further discussion in

  D. Leinweber, *et al.* JPS Conf. Proc. **10** (2016), 010011 [arXiv:1511.09146 [hep-lat]].

Other Calculations of the Nucleon Spectrum

- Cyprus Twisted Mass and Clover Fermion results

  C. Alexandrou, *et al.*, Phys. Rev. D **89** (2014) no.3, 034502 [arXiv:1302.4410 [hep-lat]].

Other Calculations of the Nucleon Spectrum

- Cyprus Twisted Mass and Clover Fermion results

  C. Alexandrou, *et al.*, Phys. Rev. D **89** (2014) no.3, 034502 [arXiv:1302.4410 [hep-lat]].

- Correlation functions subsequently analysed in the Athens Model Independent Analysis Scheme (AMIAS).

  C. Alexandrou, *et al.*, Phys. Rev. D **91** (2015) no.1, 014506 [arXiv:1411.6765 [hep-lat]].

Search for low-lying lattice QCD eigenstates in the Roper regime

A. L. Kiratidis, *et al.*, [CSSM] Phys. Rev. D **95**, no. 7, 074507 (2017) [arXiv:1608.03051 [hep-lat]].